JPRS L/10069

23 October 1981

USSR Report

ELECTRONICS AND ELECTRICAL ENGINEERING

(FOUO 11/81)

FBIS FOREIGN BROADCAST INFORMATION SERVICE

FOR OFFICIAL USE ONLY

APPROVED FOR RELEASE: 2007/02/09: CIA-RDP82-00850R000400060046-1

NOTE

JPRS publications contain information primarily from foreign newspapers, periodicals and books, but also from news agency transmissions and broadcasts. Materials from foreign-language sources are translated; those from English-language sources are transcribed or reprinted, with the original phrasing and other characteristics retained.

Headlines, editorial reports, and material enclosed in brackets [] are supplied by JPRS. Processing indicators such as [Text] or [Excerpt] in the first line of each item, or following the last line of a brief, indicate how the original information was processed. Where no processing indicator is given, the information was summarized or extracted.

Unfamiliar names rendered phonetically or transliterated are enclosed in parentheses. Words or names preceded by a question mark and enclosed in parentheses were not clear in the original but have been supplied as appropriate in context. Other unattributed parenthetical notes within the body of an item originate with the source. Times within items are as given by source.

The contents of this publication in no way represent the policies, views or attitudes of the U.S. Government.

APPROVED FOR RELEASE: 2007/02/09: CIA-RDP82-00850R000400060046-1

JPRS L/10069

23 October 1981

USSR REPORT

ELECTRONICS AND ELECTRICAL ENGINEERING

(FOUO 11/81)

CONTENTS

COMMUNICATIONS, COMMUNICATION EQUIPMENT, RECEIVERS AND TRANSMITTERS, NETWORKS, RADIO PHYSICS, DATA TRANSMISSION AND PROCESSING, INFORMATION THEORY

UDC 621.391.193

DETECTION AND MEASUREMENT OF NARROW BAND RADIO SIGNAL FREQUENCY AGAINST INTERFERENCE BACKGROUND IN ACOUSTICAL OPTO-ELECTRONIC SPECTRUM ANALYZER

Kiev IZVESTIYA VYSSHIKH UCHEBNYKH ZAVEDENIY: RADIOELEKTRONIKA in Russian Vol 24, No 4, Apr 81 (manuscript received 12 May 80, after revision 14 Oct 80) pp 26-33

[Article by A.S. Gurevich and G.S. Nakhmanson]

[Text] The analysis of a narrow band radio signal and a narrow normal random process by means of an acoustical opto-electronic spectrum analyzer is treated. Expressions are derived for the detection characteristics and the statistical characteristics of estimates of the signal frequency for the case of reception against a background of external noise and internal interference from the opto-electronic system of the spectrum analyzer.

Increasing attention is being devoted to acoustical opto-electronic devices [1-4] and others at the present time in the design of optical system for information processing. Such devices are acoustical opto-electronic spectrum analyzers (AOES), which take the form of a combination of an acoustical optical processor (AOP) and an opto-electronic (OES), which perform the simultaneous analysis of the received signals in a wide range of frequency in real time. In this case, the quality of the analysis of the received signals (the detection characteristics, the precision of the measurement of the signal spectrum parameters) depends substantially on the impact of external and internal noise. One of the methods of improving signal analysis quality is the choice of the appropriate circuit configuration for the opto-electronic system.

The reception of a narrow band radio signal and a narrow band random process against a background of internal and external noise by an acoustical opto-electronic spectrum analyzer is treated in this paper, where the circuit of the analyzer is shown in Figure 1. The detection characteristics and the ultimate measurement precision for the center frequency of the spectrum of the received signals are analyzed.

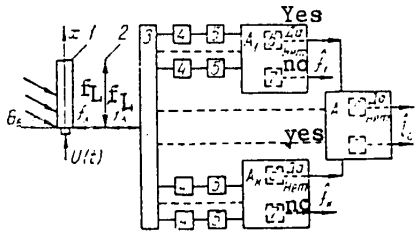

Figure 1.

The acoustical-optical processor, AOES, which is shown in Figure 1 consists of an ultrasonic light modulator (UZMS), a device for information input to the AOES, 1, and an integrating lens, 2, with a focal distance of f_L. The optical signals in the output plane of the acoustical-optical processor are registered and processed by the opto-electronic system, which consists of an opto-electronic transducer (OEP), 3, which is a linear matrix of photodetectors, which convert the optical signals to electrical ones, and an electronic processing system, which contains n channels, divided in k groups. Each working channel of the electronic system contains an OEP photodetector 3, amplifier 4 and a threshold gate 5. The actuation level of the threshold gates in each of the k groups can be set at various levels in the general case depending on the noise level in the range of frequencies corresponding to the given group of channels. The output signals of the threshold gates within each groups are fed to the input of a group resolver Ai (i = 1, ..., k), which contains a detector unit 6 and a frequency measurement unit 7. The detection unit of the resolver for the i-th group sums the output signals of the groups channels and makes a decision concerning the presence of a signal in the case of the actuation of the threshold gate in any of the channels. The frequency measurment unit sums the output signals of the threshold gates with a "weight", which is proportional to the number of the channel figured from the beginning of the group. The measurement of the frequency of the received signals in a limited frequency range (within a group) makes it possible when receiving signals against a background of strong noise to reduce the probability of anomalous errors, which increase with an increase in the apriori specified frequency range [5]. Resolver A makes a decision concerning the presence of the received signal in the range of frequencies corresponding to the given group of photodetectors, based on the "weighted" summing of the output signals of the group resolvers.

Let the following additive mixture be fed to the input of the ultrasonic light modulator of the acoustical-optical electronic spectrum analyzer:

$$x(t) = s(t) + n(t), \tag{1}$$

where $s(t) = \mathrm{Re}\{a_0 \dot{U}(t) \exp j(\omega_0 t + \varphi)\}$ is a narrow band radio signal with the complex envelope $\dot{U}(t) = U(t)e^{j\Phi(t)}$, while $n(t) = \mathrm{Re}\{\dot{N}(t)e^{j\omega_\pi t}\}$ is normal noise with a zero mean value and a correlation function of $B(\tau) = 1/2\,\mathrm{Re}\{\dot{B}(\tau)e^{j\omega_\pi \tau}\}$; $\dot{B}(\tau) = \langle \dot{N}(t)\dot{N}(t+\tau)\rangle$. Then the distribution of the light field intensity in the output focal plane (ξ, η) of the integrating lens with a focal distance of f_L can be represented in the following form [4] as a function of the spatial frequencies $u = \frac{2\pi}{\lambda}\sin\theta_B - \frac{2\pi\xi}{\lambda f_n}$ and $v = -\frac{2\pi\eta}{\lambda f_n}$

$$I(u, v, t) = I_s(u, v, t) + I_n(u, v, t), \tag{2}$$

where

$$I_s(u, v, t) = \left(\frac{E_0 \psi H}{\lambda f_n}\right)^2 \operatorname{sinc}^2 \frac{vH}{2} \left| a_0 \int_0^D \dot{U}\left(t - \frac{x}{V}\right) e^{i\left(u - \frac{\omega_0}{V}\right)x} dx \right|^2 \tag{3}$$

is the signal component of the intensity which carries the useful information on the parameters of the received signal;

$$I_n(u, v, t) = \left(\frac{E_0 \psi H}{2}\right)^2 \operatorname{sinc}^2 \frac{vH}{2} \left\{ \left| \int_0^D \dot{N}\left(t - \frac{x}{V}\right) e^{i\left(u - \frac{\omega_n}{V}\right)x} dx \right|^2 + \right.$$

$$\left. + 2 \operatorname{Re}\left[e^{i[(\omega_0 - \omega_n)t + \varphi]} \int_0^D a_0 \dot{U}\left(t - \frac{x}{V}\right) e^{i\left(u - \frac{\omega_0}{V}\right)x} dx \int_0^D \dot{N}\left(t - \frac{x}{V}\right) e^{-i\left(u - \frac{\omega_n}{V}\right)x} dx \right] \right\} \tag{4}$$

(4)

is the interference component of the intensity, the statistical characteristics of which, the mean value and the correlation function, have the form:

$$\langle I_n(u, v, t) \rangle = \left(\frac{E_0 \psi H}{\lambda f_n}\right)^2 \operatorname{sinc}^2 \frac{vH}{2} \int_0^D \int_0^D \dot{B}\left(\frac{x_1 - x_2}{V}\right) e^{i\left(u - \frac{\omega_n}{V}\right)(x_1 - x_2)} dx_1 dx_2, \tag{5}$$

$$B_I(u_1, u_2, v_1, v_2, t_1, t_2) = \left(\frac{E_0 \psi H}{\lambda f_n}\right)^4 \operatorname{sinc}^2 \frac{v_1 H}{2} \operatorname{sinc}^2 \frac{v_2 H}{2} \times$$

$$\times \left\{ \int_0^D \int_0^D \int_0^D \int_0^D \dot{B}\left(t_1 - t_2 - \frac{x_2 - x_3}{V}\right) \dot{B}\left(t_1 - t_2 - \frac{x_1 - x_4}{V}\right) \times \right.$$

$$\times e^{i\left(u_1 - \frac{\omega_n}{V}\right)(x_1 - x_2) - i\left(u_2 - \frac{\omega_n}{V}\right)(x_3 - x_4)} dx_1 dx_2 dx_3 dx_4 + 2 \operatorname{Re}\left[e^{-i(\omega_0 - \omega_n)(t_1 - t_2)} \times \right.$$

$$\times \int_0^D a_0 \dot{U}\left(t_1 - \frac{x}{V}\right) e^{-i\left(u_1 - \frac{\omega_0}{V}\right)x} dx \int_0^D a_0 \dot{U}\left(t_2 - \frac{x}{V}\right) e^{i\left(u_2 - \frac{\omega_0}{V}\right)x} dx \times$$

$$\left. \left. \times \int_0^D \int_0^D \dot{B}\left(t_1 - t_2 - \frac{x_1 - x_2}{V}\right) e^{i\left(u_1 - \frac{\omega_n}{V}\right)x_1 - i\left(u_2 - \frac{\omega_n}{V}\right)x_2} dx_1 dx_2 \right] \right\}. \tag{6}$$

It is presupposed in expressions (3)-(6) and the subsequent discussion that the duration of s(t) considerably exceeds the time it takes the signal to pass through the aperature of the ultrasonic light modulator, and the analysis is made for the case of complete filling of the light modulator.

When receiving a narrow band normal random process with a zero mean value and a spectral density of $S(\omega-\omega_0)$, which is concentrated in the vicinity of ω_0, the expressions for the statistical characteristics of the intensity distribution in the plane (ξ, η) which can be derived on analogy with [3, 4] have the form:

$$\langle I_s(u, v, t)\rangle = \left(\frac{E_0\psi HD}{\lambda f_n}\right)^2 \operatorname{sinc}^2\frac{vH}{2}\,\frac{\sigma_0^2}{2}\left[\operatorname{sinc}^2\frac{D}{2}\left(u+\frac{\omega_0}{V}\right)+\right.$$
$$\left.+\operatorname{sinc}^2\frac{D}{2}\left(u-\frac{\omega_0}{V}\right)\right], \qquad (7)$$

$$B(u_1, u_2, v_1, v_2, t_1, t_2) = \left(\frac{E_0\psi HD}{\lambda f_n}\right)^4 \operatorname{sinc}^2\frac{v_1H}{2}\operatorname{sinc}^2\frac{v_2H}{2}\left\{\frac{\sigma_0^4}{4}\{[(d_1^-)^2+\right.$$
$$+(d_1^+)^2][(d_2^-)^2+(d_2^+)^2]+4d_1^-d_1^+d_2^-d_2^+\cos 2\omega_0(t_1-t_2)\}+$$
$$+\frac{1}{D^2}\int_0^D\int\int\dot{B}\left(t_1-t_2-\frac{x_1-x_4}{V}\right)\dot{B}\left(t_1-t_2-\frac{x_2-x_3}{V}\right)\times$$
$$\times e^{j\left[\left(u_1-\frac{\omega_n}{V}\right)(x_1-x_2)-\left(u_2-\frac{\omega_n}{V}\right)(x_3-x_4)\right]}dx_1dx_2dx_3dx_4+$$
$$+\frac{\sigma_0^2}{D^2}\operatorname{Re}\left\{[d_1^-d_2^-e^{j\left[(\omega_0+\omega_n)(t_1-t_2)+(u_1-u_2)\frac{D}{2}\right]}+d_1^+d_2^+e^{j(\omega_n-\omega_0)(t_1-t_2)}\times\right.$$
$$\left.\times e^{j(u_1-u_2)\frac{D}{2}}]\int_0^D\int\dot{B}\left(t_1-t_2-\frac{x_1-x_2}{V}\right)e^{-j\left[\left(u_1-\frac{\omega_n}{V}\right)x_1-\left(u_2-\frac{\omega_n}{V}\right)x_2\right]}dx_1dx_2\right\}, \qquad (8)$$

где where

$$d_i^{\pm}=\operatorname{sinc}\frac{D}{2}\left(u_i\pm\frac{\omega_0}{V}\right), \qquad \sigma_0^2=\frac{1}{2\pi}\int_0^{\infty}S(\omega-\omega_0)\,d\omega.$$

The mean value of the interference component $\langle I_{\pi}(u,v,t)\rangle$, as follows from expression (5), is a steady-state quantity and can be compensated in subsequent opto-electronic processing at the output of the opto-electronic transducer [4]. For this reason, it can be assumed in the following that it is equal to zero without losing any generality.

The conversion of optical signals to electrical ones, as was indicated above, is accomplished in the (ξ, η) plane by means of the photodetectors of the

opto-electronic transducer having dimensions of d_ξ x d_η each, the centers of which are spaced along the O_ξ axis at resolution intervals of $\Delta\xi = \lambda f_L/D$. Then the electrical signal at the output of the photodetector of the r-th group having center coordinates of $\xi_i = i\Delta\xi$ can be represented in the following manner:

$$G_i^{(r)}(t) = K_{\text{пр}} \int_{\xi_i - \frac{d_\xi}{2}}^{\xi_i + \frac{d_\xi}{2}} d\xi \int_{-d_\eta/2}^{d_\eta/2} d\eta I(u, v, t) + n_{\text{ш}i}(t), \tag{9}$$

where $K_{\text{пр}}$ is the slope of the characteristic of the photodetector; $n_{\text{ш}i}(t)$ is the internal noise of the photodetector and the amplifier following it, refigured for the input of the latter, which have a zero mean value and a correlation function of $\langle n_{\text{ш}i}(t_1) n_{\text{ш}j}(t_2)\rangle = N_{\text{ш}} 2\delta(t_1 - t_2)\delta_{ij}$; δ_{ij} is Kronecker's delta; $\delta(t_1 - t_2)$ is a delta function. In the case of Bragg diffraction, the following inequality is usually justified: $d_\xi D/\lambda f_L \ll 1$. In this case, the expression for $G_i^{(r)}$ can be represented thusly:

$$G_i^{(r)}(t) = \varkappa I(u_i^{(r)}, 0, t) + n_{\text{ш}i}(t), \quad \varkappa = K_{\text{пр}} d_\xi d_\eta. \tag{10}$$

Then the signal to the input of the threshold gate can be written as:

$$p_i^{(r)}(t) = \int_{t_{\text{н}}}^{t} G_i^{(r)}(t - \tau) h(\tau)\, d\tau, \tag{11}$$

where $h(t) = \Delta f e^{-\Delta f t}$ is the pulse characteristic of one channel; $t_H = T_M = D/V$ is the moment of the start of registration, corresponding to the filling of the aperture of the ultrasonic light modulator with the signal being analyzed. The expressions which describe the output effects of the detection unit and the frequency estimation unit of the resolver A_r of the r-th group, have the form:

$$Z_r(t) = \xi_1^{(r)}(t)\, V \xi_2^{(r)} V \ldots V \xi_{n_r}^{(r)}(t), \tag{12}$$

$$\hat{f}_r = \frac{\Delta\omega_r}{2\pi n_r} \sum_{i=1}^{n_r} i\xi_i^{(r)}(t), \qquad \xi_i^{(r)}(t) = \begin{cases} 1, & p_i^{(r)}(t) \gtrless \gamma_r \\ 0, & \end{cases} \tag{13}$$

where $\Delta\omega_r$ is the apriori value of the r-th frequency interval, while V designates the operation of logic addition. The output signals of the detection and interval number estimation units, in which the signal is received, and of the resolver A, are written in the following manner:

$$B = Z_1(t)\, V Z_2(t)\, V \ldots V Z_\kappa(t), \tag{14}$$

$$\hat{l} = \sum_{r=1}^{\kappa} r Z_r(t), \tag{15}$$

where

$$Z_r(t) = \begin{cases} 1, \sum_{i=1}^{n_r} \xi_i^{(r)}(t) \geqslant 1, \\ 0, \sum_{i=1}^{n_r} \xi_i^{(r)}(t) = 0, \end{cases}$$

i.e., the decision is made that a signal has appeared in the r-th interval when $Z_r(t) > Z_{thresh}$ and that there is no signal when $Z_r(t) < Z_{thresh}$. We shall consider the detection characteristics and the statistical characteristics of the estimates of the frequency and the frequency range when a signal is received in the j-th frequency interval.

If the hypothesis H_j (j = 1, ..., k) consists in the fact that the signal being analyzed belongs to the j-th frequency interval, the expressions for the false alarm probability and the probability of missing a signal (given the condition that the hypothesis H_j is correct) can be written as:

$$P_{f.a.} = P_{\text{л.т}} = 1 - \int_{-\infty}^{\gamma_1} \cdots \int \cdots \int_{-\infty}^{\gamma_k} \cdots \int W_{n_1+n_2+\ldots+n_k}(\vec{p}/s = 0)\, d\vec{p}, \tag{16}$$

$$P_j = \int_{-\infty}^{\gamma_j} \cdots \int W_{n_j}(\vec{p}/s \neq 0)\, d\vec{p}, \tag{17}$$

where γ_j is the level of the threshold at the output of the working channels of the j-th group; $W_{n_1+n_2+\ldots+n_k}(\vec{p}/s = 0)$ is the combined probability density of the output effects of the working channels of the opto-electronic system at the input to the threshold gates when no signal is present; $W_{nj}(\vec{p}/s \neq 0)$ is the combined probability density of the output effects of the working channels of the j-th group of the opto-electronic system at the input to the threshold gate when a signal is present, where the signal being received belongs to the j-th frequency interval, and the probability of an erroneous decision when the hypothesis H_j is correct is:

$$P_{\substack{\text{ош} \\ \text{error}}}(H_j) = \sum_{r \neq j}^{\kappa} \left[1 - \int_{-\infty}^{\gamma_r} \cdots \int W_{n_r}(\vec{p}/s = 0)\, d\vec{p} + \right] \int_{-\infty}^{\gamma_j} \cdots \int W_{n_j}(\vec{p}/s \neq 0)\, d\vec{p}. \tag{18}$$

The expressions for the biases and dispersions of the estimates of the signal frequency and the frequency interval to the which the signal belongs is written as follows:

$$\langle \hat{f} \rangle = \frac{\Delta\omega_r}{2\pi n_r} \sum_{i=1}^{n_r} iD_i^{(r)}, \tag{19}$$

$$\sigma_f^2 = \frac{\Delta\omega_r^2}{4\pi^2 n_r^2} \sum_{i=1}^{n_r} \sum_{j=1}^{n_r} ij\,[D_{ij}^{(r)} - D_i^{(r)} D_j^{(r)}], \tag{20}$$

$$\langle \hat{l} \rangle = \sum_{r=1}^{k} r\,\langle Z_r(t) \rangle = \sum_{r=1}^{\kappa} rD_r, \tag{21}$$

$$\sigma_l^2 = \sum_{r=1}^{\kappa} \sum_{j=1}^{\kappa} rj\,[D_{rj} - D_r D_j], \tag{22}$$

$$D_i^{(r)} = \int_{\gamma_r}^{\infty} W(p_i^{(r)})\,dp_i^{(r)}, \qquad D_r = 1 - \int_{-\infty}^{\gamma_r} \cdots \int W_{n_r}(\vec{p})\,d\vec{p} \tag{23}$$

are the probabilities that the threshold is exceeded at the output of the i-th channel of the r-th group and at the output of the threshold gate of the r-th group respectively, while:

$$W_{ij}^{(r)} = \int_{\gamma_r}^{\infty} \cdots \int W(p_i^{(r)}, p_j^{(r)})\,dp_i^{(r)} dp_j^{(r)} \tag{24}$$

is the probability that the threshold is exceeded simultaneously at the output of the i-th and j-th channels of the r-th group.

$$D_{rj} = 1 + \int_{-\infty}^{\gamma_r} \cdots \int \int_{-\infty}^{\gamma_j} \cdots \int W_{n_r+n_j}(\vec{p})\,d\vec{p} - \int_{-\infty}^{\gamma_r} \cdots \int W_{n_r}(\vec{p})\,d\vec{p} - \int_{-\infty}^{\gamma_j} \cdots \int W_{n_j}(\vec{p})\,d\vec{p} \tag{25}$$

is the probability that the thresholds of the r-th and j-th group resolvers are exceeded together; $W(p_i^{(r)}, p_j^{(r)})$ is the combined probability density of the values of $p_i^{(r)}$ and $p_j^{(r)}$ at the output of the i-th and j-th channels of the r-th group; $W_{n_r+n_j}(\vec{p}) = W(p_1^{(r)}, \ldots, p_{n_r}^{(r)}, p_1^{(j)}, \ldots, p_{n_j}^{(j)})$ is the combined probability density of the values of the output signals in the channels of the r-th and j-th groups. Considering the fact that a narrow band signal is applied to the input of the acoustical opto-electronic spectrum analyzer, while the photodetectors are spaced along the O_ξ axis at distances equal to the resolution elements $\Delta\xi$, the expressions for the statistical detection characteristics, the estimates of the center frequency of the signal and the number of the frequency interval to the which the received signal belongs, (16)-(22) can be written as:

$$P_{\text{лт}} = 1 - \prod_{i=1}^{\kappa} \Phi^{n_i}(a_\lambda^i), \quad \lambda = 1, \ldots, n_i,$$

$$P_{l_0} = \Phi^{n_{l_0}-1}(a_i^{l_0})\,\Phi(a_{i_0}^{l_0}), \quad i = 1, \ldots, n_{l_0},$$

$$P_{\text{ош}}(H_{l_0}) = \sum_{r \neq l_0}^{\kappa} [1 - \Phi^{n_r}(a_i^r)] + \Phi^{n_{l_0}-1}(a_i^{l_0})\,\Phi(a_{i_0}^{l_0}),$$

$$\frac{\langle \hat{f} - f_0 \rangle}{f_0} = \frac{n_{l_0}(n_{l_0}+1)}{2i_0}[1 - \Phi(a_i^{l_0})] + \Phi(a_i^{l_0}) - \Phi(a_{i_0}^{l_0}) - 1,$$

$$\frac{\sigma_f^2}{f_0^2} = \frac{n_{l_0}(n_{l_0}+1)(2n_{l_0}+1)}{2i_0^2}\,\Phi(a_i^{l_0})[1 - \Phi(a_i^{l_0})] + \Phi(a_{i_0}^{l_0})[1 - \Phi(a_{i_0}^{l_0})],$$

$$\frac{\langle \hat{l} - l_0 \rangle}{l_0} = \frac{1}{l_0} \sum_{r \neq l_0}^{\kappa} r[1 - \Phi^{n_r}(a_i^r)] - \Phi^{n_{l_0}-1}(a_i^{l_0})\,\Phi(a_{i_0}^{l_0}),$$

$$\frac{\sigma_l^2}{l_0^2} = \Phi^{n_{l_0}-1}(a_i^{l_0})\,\Phi(a_{i_0}^{l_0})[1 - \Phi^{n_{l_0}-1}(a_i^{l_0})\,\Phi(a_{i_0}^{l_0})] + \frac{1}{l_0^2} \sum_{r \neq l_0}^{\kappa} r^2 \Phi^{n_r}(a_i^r) \times$$

$$\times [1 - \Phi^{n_r}(a_i^r)],$$

where $\mathcal{I}_0$ is the frequency interval in which the signal is received; i_0 is the number of the responding channel within the interval $\mathcal{I}_0$; $\Phi(x)$ is the probability integral of [6];

$$a_1^{l_0} = \ldots = a_{n_{l_0}}^{l_0} \overset{\text{when}}{\text{при}}\ i \neq i_0,\ a_1^r = \ldots = a_{n_r}^r = a_i^r \overset{\text{when}}{\text{при}}\ r \neq l_0;\ a_i^{(r)} = \frac{\gamma_{\text{пор}} - m_i^{(r)}}{\sigma_i^{(r)}},$$

$\sigma_i^{(r)} = [\rho_{ii}^{(r)}]^{\frac{1}{2}}$ for all i and j of the r-th group;

$$\Gamma_{ij}^{(r)} = \langle p_i^{(r)}(T)\, p_j^{(r)}(T) \rangle - m_i^{(r)} m_j^{(r)} = \int_{t_{\text{н}}}^{T}\int B_{ij}^{(r)}(t_1, t_2)\, h(T - t_1)\, h(T - t_2)\, dt_1 dt_2,$$

$$B_{ij}^{(r)}(t_1, t_2) = \varkappa^2 [\langle I(u_i^{(r)}, 0, t_1)\, I(u_j^{(r)}, 0, t_2) \rangle - \langle I(u_i^{(r)}, 0, t_1) \rangle \times$$

$$\times \langle I(u_j^{(r)}, 0, t_2) \rangle] + \frac{N_{\text{ш}}}{2}\,\delta(t_1 - t_2)\,\delta_{ij},$$

$$m_i^{(r)} = \langle p_i^{(r)}(T) \rangle = \varkappa \int_{t_{\text{н}}}^{T} \langle I_{\text{с}}(u_i^{(r)}, 0, t) \rangle\, h(T - t)\, dt,$$

$B_{ij}^{(r)}$ and $\rho_{ij}^{(r)}$ are the correlation functions of the signals at the input of the i-th and j-th channels of the r-th group; $m_i^{(r)}$ is the mean value of the signal at the output of the i-th channel of the r-th group.

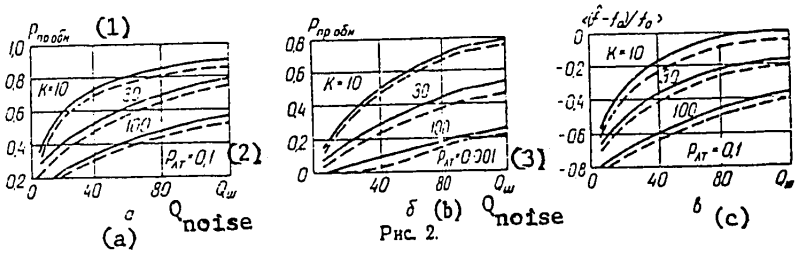

Рис. 2.

Figure 2.

Key: 1. Detection probability.

To illustrate the results, we shall consider the reception of a square-wave narrow band radio signal, $s(t) = a_0\cos(\omega_0 t + \phi)$ with a width of $\tau_S >> T_M = D/V$ and a narrow band normal random process, the spectral density of which is concentrated in the vicinity of the frequency s_0, against a background of white noise with a spectral density of N_0 and the internal noise of the opto-electronic system with a spectral density of $N_Ш$. It is assumed in this case that the opto-electronic system contains 100 working channels, broken down into 10 groups, in which case, if it is considered that the spectral noise density along the entire frequency is constant, the threshold level at the output of the working channel γ_r is chosen the same. The calculations of the detection characteristics and the statistical characteristics of the estimates of the signal frequency and the number of the frequency interval to which the received signal belongs were made for the following values of the parameters: a false alarm probability $P_{s.a.}$ = = 0.1 and 0.001; a coefficient of $K = \left[\varkappa\left(\frac{E_0\psi HD}{\lambda f_л}\right)^2 \frac{N_0}{T_м}/\sqrt{N_ш\Delta f}\right]^2$ = 10, 30 and 100 - the ratios of the referenced internal and external noise powers; $Q_{noise} = Q_ш =$ $= \frac{m_{i0}^2}{N_ш\Delta f} = \varkappa^2\left[E_0\psi\frac{HD}{\lambda f_л}\right]^4 \times (N_ш\Delta f)^{-1}$ = 5 to 200 - the signal/internal noise ratio.

The curves for the detection probability P_{det} are shown in Figures 2a, b and c as functions of the signal/noise ratio Q_{noise} for various values of the ratio of the external and internal noise power and the false alarm probability $P_{f.a.}$. The solid curves correspond to the reception of a determinate signal, while the dashed curves apply to the random process. It can be seen from the nature of the curves that the detection probability increases with an increase in the signal/noise ratio Q_{noise} and with a decrease in k (a reduction in the external interference power at the input). In the case of an unchanged signal/noise ratio Q_{noise}, an increase in k leads to a reduction in the output signal/noise ratio, and correspondingly to a decrease in the detection probability. With a reduction in the false alarm probability, the level of the threshold rises, and

for this reason, to retain a specified detection probability, it is necessary to increase the signal power.

The curves for the relative bias in the estimate of the frequency $\langle \hat{f} - f_0 \rangle f_0$ and the dispersion σ_f^2/f_0^2 are shown in Figures 3a, b and c as a function of Q_0 for values of k and $P_{f.a.}$. It follows from the nature of the curves in Figures 2c and 3a that the value of the frequency estimate bias depends substantially on the false alarm probability and the ratio of the external and internal noise powers. In this case, when k > 10, the value of the bias falls off with an increase in the signal/noise ratio. As follows from the nature of the curves in Figures 3b and 3c, the value of the frequency estimate dispersion has a sharply pronounced maximum, which shifts with an increase in k to the region of greater signal/noise ratios. This can be explained in the following manner: with an increase in the signal power (when the useful signal power is considerably less than the external noise power), the noise component of the intensity at the input to the opto-electronic system, which is due to the interaction of the signal and the external noise, increases more rapidly than does the useful component of the intensity and the value of the frequency estimate dispersion increases. In step with the useful signal compoents starting to exceed the interference components, the level of the dispersion reaches a maximum and thereafter begins to fall off.

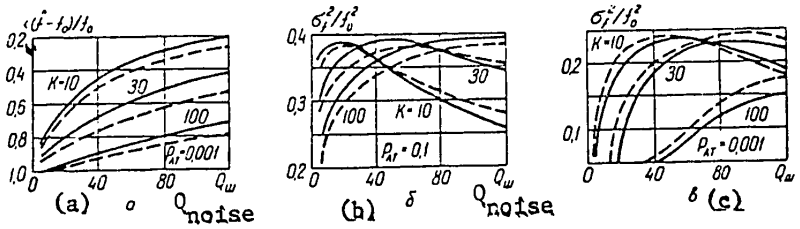

Figure 3.

In this case, the greater the external noise power (k increases), the greater the signal/noise ratio at which the maximum of the dispersion is achieved. When the false alarm probability is reduced (i.e., the threshold level increased), the power of the interference spikes decreases, and for this reason, the level of the maximum value of the estimate dispersion is reduced. As calculations demonstrate, the nature of the curves of the statistical characteristics of the estimates of the number of the frequency interval to which the received signal belongs, is similar to the behavior of the statistical characteristics of the estimate of the frequency of the signals being analyzed, and therefore, these functions are not given here.

BIBLIOGRAPHY

1. Parks, "Akustoopticheskiy priyemnik-spektroanalizator detsimetrovogo diapazona" ["An Acoustical-Optical Receiver-Spectrum Analyzer for the Decimeter Band"], ZARUBEZHNAYA RADIOELEKTRONIKA [FOREIGN RADIOELECTRONICS], 1970, No 12, p 14.

2. Kulakov S.V., "Akustoopticheskiy ustroystva spektral'nogo i korrelyatsionnogo analiza signalov" ["Acoustical-Optical Devices for Spectral and Correlation Signal Analysis"], Moscow, Nauka Publishers, 1978.

3. Drakin Ye.V., Auslender A.L., "K raschetu rabochikh kharakteristik opticheskogo spektroanalizatora s fazovoy modulyatsiyey kogerentnogo svetovogo potoka" ["On the Calculation of the Operating Characteristics of an Optical Spectrum Analyzer with Phase Modulation of the coherent Light Flux"], VOPROSY RADIOELEKTRONIKI [QUESTIONS IN RADIOELECTRONICS], Seriya Obshchetekhnicheskaya ["General Engineering Series"], 1974, No 8, p 56.

4. Nakhmanson G.S., "Tochnost' izmereniya chastoty i ugla prikhoda signalov, prinimayemykh antennoy reshetkoy na fone pomekh pri akustoopticheskoy obrabotke" ["The Precision in the Measurement of the Frequency and Incident Angle of Signals Received by an Antenna Array against a Background of Interference in the case of Acoustical-Optical Processing"], IZV. VUZOV. RADIOELEKTRONIKA [PROCEEDINGS OF THE HIGHER EDUCATIONAL INSTITUTES. RADIOELECTRONICS], 1980, 23, No 1, pp 3-10.

5. Fomin A.F., "Pomekhoustoychivost' sistem peredachi nepreryvnykh soobshcheniy" ["The Interference Immunity of Discrete Message Transmission Systems"], Moscow, Sovetskoye Radio Publishers, 1915 [sic].

6. Tikhonov V.I., "Statisticheskaya radiotekhnika"["Statistical Radio Engineering"], Moscow, Sovetskoye Radio Publishers, 1966.

8225
CSO: 1860/327

UDC 621.391.193

PRECISE MEASURING OF RADIO SIGNAL CARRIER FREQUENCY AT OUTPUT OF ACOUSTICAL-OPTICAL FREQUENCY GATE IN PRESENCE OF EXTERNAL ADDITIVE INTERFERENCE

Kiev IZVESTIYA VYSSHIKH UCHEBNYKH ZAVEDENIY: RADIOELEKTRONIKA in Russian Vol 24, No 4, Apr 81 (manuscript received 21 Dec 79) pp 46-52

[Paper by B.G. Katkov]

[Text] It is shown that when a mixture of a signal and noise pass through an acoustical-optical frequency gate, a multiplicative component appears in the output signal. Expressions to estimate the precision in measuring the carrier frequency of radio signals are derived and analyzed.

We shall consider the impact of external additive interference on the precision of the measurement of the carrier frequency of radio signals passing through a gating deivce designed around an acoustical-optical (AO) parametric four-pole network, the generalized schematic of which is depicted in Figure 1. We shall assume in this case that the receiving and analyzing equipment is optical for the measurement of the radio signal carrier frequency against a background of whitenoise.

We shall assume that the input signal $s_1(t) = \mathrm{Re}\{\dot{s}_1(t)\}$, which is fed to the first ultrasonic light modulator (UZMS1), takes the form of an additive mixture of the signal $s(t)\mathrm{Re}\{\dot{s}(t)\}$ and interference $n(t) = \mathrm{Re}\{\dot{n}(t)\}$, while a reference signal $s_2(t) = \mathrm{Re}\{\dot{s}_2(t)\}$ is fed to the input of UZMS2 [ultrasonic light modulator 2].

Let ultrasonic light modulators 1 and 2 operate in a Raman--Nata diffraction mode. It is easy to show [1] that in this case, the monochromatic light wave having a plane front, a frequency of ω_{CB} and an amplitude of E_0, which is normally incident to ultrasonic light modulator 1, and passes through lenses L_1 and L_2, as well as the spatial frequency filter Φ and ultrasonic light modulator 2, will produce a light distribution in the focal plane of integrating lens L_3 which can be described by the expression:

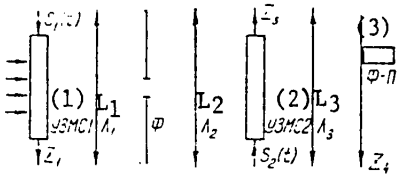

Figure 1.

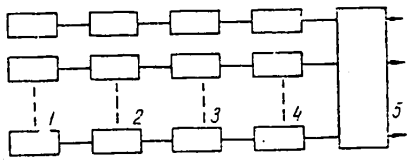

Figure 2.

Key: 1. UZMS 1 [ultrasonic light modulator 1];
2. Ultrasonic light modulator 2;
3. Photodetector.

$$e(t, \omega_z) \simeq E_0 \lambda F_1 \operatorname{Re}\left\{\exp(j\omega_{c_2} t) \int_{-\infty}^{\infty}\left[r(z_3) A_1 \dot{s}_1\left(V_1 t - \frac{1}{P} z_3\right) + r(z_3) A_2 \dot{s}_2\left(\frac{V_1 t + Q z_3}{Q}\right)\right] \exp(-j\omega_z z_3)\, dz_3\right\}, \quad (1)$$

where $\omega_z = -(2\pi/\lambda F_3) z_4$; λ is the wavelength of the light; F_1, F_2 and F_3 are the focal lengths of the lenses L_1, L_2 and L_3; $P = F_2/F_1$; $Q = V_1/V_2$, V_1 and V_2 are the propagation velocities of the ultrasound in ultrasonic light modulators 1 and 2; A_1 and A_2 are coefficients which determine the level of modulation of the light flux in ultrasonic light modulators 1 and 2;

$$r(z_3) \equiv r_1^2\left(\frac{1}{P z_3}\right) r_2(z_3) \equiv r_1\left(\frac{1}{P z_3}\right) r_2^2(z_3);$$

$r(z) = \begin{cases} 1, & |z| < 0{,}5L \\ 0, & |z| > 0{,}5L \end{cases}$, L is the aperture of the ultrasonic light modulators; r_1 and r_2 are the aperture functions of ultrasonic light modulators 1 and 2.

To simplify the mathematical derivations, we shall assume that the light distribution along the z_4 coordinate is registered by means of one photodetector with a square-law response. In this case, the expression for the output current of the photodetector can be written in the form:

$$i_s(t) \simeq B_1'(E_0 \lambda F_1 A_2)^2 \int_G \left| \int_{-\infty}^{\infty} r(z_3)\, \dot{s}_1\left(V_1 t - \frac{z_3}{P}\right) \exp(-j\omega_z z_3)\, dz_3 \right|^2 dz_4 + B_1(E_0 \lambda F_1 A_1)^2 \int_G \left| \int_{-\infty}^{\infty} r(z_3)\, \dot{s}_2\left(\frac{V_1 t + Q z_3}{Q}\right) \exp(-j\omega_z z_3)\, dz_3 \right|^2 dz_4 + \quad (2)$$

$$+ 2B_1 (E_0 \lambda F_1)^2 A_1 A_2 \int_G \left| \int_{-\infty}^{\infty} r(z_3)\, \dot{s}_2\left(\frac{V_1 t + Qz_3}{Q}\right) \exp(-j\omega_2 z_3)\, dz_3 \right| \times$$
$$\times \left| \int_{-\infty}^{\infty} r(z_3)\, \dot{s}_1\left(V_1 t - \frac{z_3}{P}\right) \exp(-j\omega_2 z_3)\, dz_3 \right| dz_4,$$

where B1 is a dimensional proportionality factor; G is the size of the input aperture of the photodetector.

In the absence of interference, the first and second terms in (2) describe slowly timewise changing electrical signals, which can be filtered out electrically (in the load of the photodetector). The third term in (2) (we shall designate it as i3(t)), which describes the useful component of the output current, can be represented in the form:

$$i_3(t) \simeq B_2 \lambda F_3 \operatorname{Re}\left\{ \int_{-\infty}^{\infty} r(z_3)\, r(-z_3)\, \dot{s}_1\left(V_1 t - \frac{z_3}{P}\right) \dot{s}_2\left(\frac{V_1 t - Qz_3}{Q}\right) dz_3 \right\}, \tag{3}$$

where $B_2 = B_1 (E_0 \lambda F_1)^2 A_1 A_2$.

In order to restore the input signal at the output of the photodetector, it is necessary to take a δ-function as the reference signal:

$$s_2\left(\frac{V_1 t - Qz_3}{Q}\right) = \delta\left(\frac{V_1 t - Qz_3}{Q}\right).$$

Then, considering that r(z3) = r(-z3) = 1, and by selecting the parameters of the four-pole network in the appropriate manner, we obtain:

$$i_3(t) \simeq B_2 \lambda F_3 \operatorname{Re}\{\dot{s}_1(t)\}, \tag{4}$$

i.e., the current spectrum of the signal s(t) is produced at each point in time along the coordinate z4 and the input signal is restored from the output of the photodector. In practice, one can take a sufficiently short pulse with a wide spectrum instead of the δ-function.

We now consider the expression for the photodetector output current in the presence of additive interference:

$$i_{an}(t) \simeq B_1 (E_0 \lambda F_1 A_1)^2 \int_G \left| \int_{-\infty}^{\infty} r(z_3) \left[\dot{s}\left(V_1 t - \frac{z_3}{P}\right) + \dot{n}\left(V_1 t - \frac{z_3}{P}\right) \right] \times \right.$$

$$\times \exp(-j\omega_z z_3)\, dz_3 \Big|^2 dz_4 + B_1 (E_0 \lambda F_1 A_2)^2 \int_G \left| \int_{-\infty}^{\infty} \dot{r}(z_3)\, \dot{s}_2\left(\frac{V_1 t + Qz_3}{Q}\right) \times \right.$$

$$\times \exp(-j\omega_z z_3)\, dz_3 \Big|^2 dz_4 + 2B_1 (E_0 \lambda F_1)^2 A_1 A_2 \int_G \left| \int_{-\infty}^{\infty} r(z_3) \left[\dot{s}_1\left(V_1 t - \frac{z_3}{P}\right) + \right. \right.$$

$$\left. \left. + \dot{n}\left(V_1 t - \frac{z_3}{P}\right) \right] \exp(-j\omega_z z_3)\, dz_3 \right| \left| \int_{-\infty}^{\infty} r(z_3)\, \dot{s}_2\left(\frac{V_1 t - Qz_3}{Q}\right) \exp(-j\omega_z z_3)\, dz_3 \right| dz_4. \qquad (5)$$

The first term in (5) can be represented in the form:

$$i_1(t) \simeq B_1 (E_0 \lambda F_1 A_1)^2 \int_G \left| \int_{-\infty}^{\infty} r(z_3)\, \dot{s}\left(V_1 t - \frac{z_3}{P}\right) \exp(-j\omega_z z_3)\, dz_3 \right|^2 dz_4 +$$

$$+ B_1 (E_0 \lambda F_1 A_1)^2 \int_G \left| \int_{-\infty}^{\infty} r(z_3)\, \dot{n}\left(V_1 t - \frac{z_3}{P}\right) \exp(-j\omega_z z_3)\, dz_3 \right|^2 dz_4 +$$

$$+ 2B_1 (E_0 \lambda F_1 A_1)^2 \int_G \left| \int_{-\infty}^{\infty} r(z_3)\, \dot{s}\left(V_1 t - \frac{z_3}{P}\right) \exp(-j\omega_z z_3)\, dz_3 \right| \times$$

$$\times \left| \int_{-\infty}^{\infty} r(z_3)\, \dot{n}\left(V_1 t - \frac{z_3}{P}\right) \exp(-j\omega_z z_3)\, dz_3 dz_4 \right|. \qquad (6)$$

Just as in (2), the first and second terms in (6) describe slowly changing functions of time. The third term in (6) can be reduced to the following form by means of simple transformations:

$$i_{13}(t) \simeq 2B_1 (E_0 \lambda F_1 A_1)^2 \lambda F_3 \operatorname{Re}\left\{ \int_{-\infty}^{\infty} r(z_3)\, r(-z_3)\, \dot{s}\left(V_1 t - \frac{z_3}{P}\right) \dot{n}\left(\frac{V_1 t - Qz_3}{Q}\right) dz_3 \right\}. \qquad (7)$$

As can be seen from (7), a multiplicative interference component will be present in the output signal. The second term in (5) describes a slowly changing

function of time. The third term in (5) (we shall designate it as $i_3(t)$) describes the sum of the input signal s(t) and the interference n(t).

Thus, when an additive mixture of a signal and interference is fed to the input of the parametric four-pole network, the restored electrical signal will contain additive and multiplicative interference components.

To realize frequency gating of the radio signals, the light field should be registered by means of photodetectors positioned along the z_4 coordinate (Figure 1) and operating in optical heterodyning mode. We shall assume that the photodetectors are placed flush against each other and the dimensions of the input apertures of the photodetectors are the same, while the size of the aperture along the z_4 c-ordinate is many times greater than the current signal spectrum. In this case, it can be assumed that at each point in time, the light fluz falls only on one photodetector.

The subsequent processing of the electrical signals from the outputs of the string of photodetectors is accomplished by means of a multichannel processor, the functional schematic of which is shown in Figure 2. The device consists of the photodetectors 1, high frequency amplifiers 2, detectors 3, threshold gates 4, resolver 5 and switcher 6. The decision that a signal is present is made in the case where the signal from the amplifier exceeds the threshold. The functions of the resolver include making a decision concerning the presence of a signal at the output of the corresponding channel of the threshold gate. The signals are fed from the outputs of the high frequency amplifiers to the receiving and analyzing equipment.

We shall assume that the internal noise of the photodetectors and amplifiers is a great deal less than the additive and multiplicative interference components, something which makes it possible to disregard this noise.

Let the input signals and the normal steady-state interference with a zero mean value be described by expressions of the form:

$$s(t) = U_0 \Pi(t) \operatorname{Re}\{\exp[j(\omega_c t + \varphi_c)]\}, \tag{9}$$

$$n(t) = \operatorname{Re}\{\dot{N}(t) \exp[j(\omega_n t + \varphi_n)]\}, \tag{10}$$

where U_0 is the signal amplitude; $\Pi(t) = \begin{cases} 1, & |t| \leqslant T \\ 0, & |t| > T \end{cases}$; T is the equivalent size of the ultrasonic light modulator aperture; ω_c and ω_n are the frequencies of the signal and the interference; $\dot{N}(t)$ is the complex amplitude of the interference.

Taking the spectral width of the interference to be much greater than the spectral width of the signal, we represent $i_{13}(t)$ in the form:

$$i_{13}(t) \simeq M_1 U_0 \Pi(t) \operatorname{Re}\{\exp[j(\omega_{zc} V_1 t + \varphi_c)] \dot{F}_1(t, \omega_z + \omega_{zc})\}, \tag{11}$$

where $\dot{F}_1(t, \omega_z + \omega_{zc}) = \int_{-\infty}^{\infty} r(z_3)\,\dot{n}\left(\frac{V_1 t - Qz_3}{Q}\right)\exp(-j\omega_z z_3)\,dz_3; \quad \omega_{zc} = \frac{\omega_c}{V_1}.$

Expression (11) can be rewritten in the form:

$$i_{13}(t) \simeq U_0 \Pi(t)\,\mathrm{Re}\{\exp[j(\omega_{zc}V_1 t + \varphi_c)]\,\dot{M}(t, \omega_z + \omega_{zc})\}, \tag{12}$$

where in accordance with [2], we shall call $M(t, \omega_z + \omega_{zc}) = \mathrm{Re}\{\dot{M}(t, \omega_z + \omega_{zc})\}$ the interference modulation function.

The correlation function of the interference modulation function $M(t, \omega_z + \omega_{zc})$ has the form:

$$B_M(\tau) \simeq 0{,}5M_1^2\,\mathrm{Re}\left\{\exp\left(j\omega_{zn}\frac{V_1\tau}{Q}\right)\int_{-0{,}5L}^{0{,}5L}\int_{-0{,}5L}^{0{,}5L}\dot{B}\left[\frac{V_1\tau - Q(z_3 - z_3')}{Q}\right]\times\right.$$
$$\exp\left[-j(z_3 - z_3')\left(\omega_z + \omega_{zn} + \frac{\omega_{zc}}{P}\right)\right]dz_3 dz_3' + \exp\left[j\left(\omega_{zn}\frac{V_1\tau}{Q} + 2\varphi_n\right)\right]\times$$
$$\left.\times\int_{-0{,}5L}^{0{,}5L}\int_{-0{,}5L}^{0{,}5L}\dot{D}\left[\frac{V_1\tau - Q(z_3 + z_3')}{Q}\right]\exp\left[-j(z_3 + z_3')\left(\omega_z + \omega_{zn} + \frac{\omega_{zc}}{P}\right)\right]dz_3 dz_3'\right. \tag{13}$$

where $\omega_{z\pi} = \omega_\pi/V_1$; $B(\tau) = \mathrm{Re}\{\dot{B}(\tau)\}$ is the interference correlation function; $D(\tau) = \mathrm{Re}\{\dot{D}(t)\}$ is the mathematical mean value of the expression $\mathrm{Re}\{\dot{N}(t)(t-\tau)\}$.

If the distribution function for the phase distortion is close to uniform in a range of $[0, 2\pi]$ (this is usually the case), then the function $D(\tau)$ is close to 0 [2] and the second term in (13) can be disregarded. Then:

$$B_M(\tau) \simeq 0{,}5M_1^2\,\mathrm{Re}\left\{\exp\left(j\omega_{zn}\frac{V_1\tau}{Q}\right)\int_{-0{,}5L}^{0{,}5L}\int_{-0{,}5L}^{0{,}5L}\dot{B}\left[\frac{V_1\tau - Q(z_3 - z_3')}{Q}\right]\times\right.$$
$$\left.\times\exp\left[-j(z_3 - z_3')\left(\omega_z + \omega_{zn} + \frac{\omega_{zc}}{P}\right)\right]dz_3 dz_3'\right\}. \tag{14}$$

Utilizing (14) and assuming that the radio signal is received against a background of white noise, we shall find the expression for the energy spectrum of the interference modulation function:

$$G_M(\omega_z) \simeq 2M_1^2 N_0 \frac{Q}{V_1}\left|\frac{\sin[0{,}5L\omega_z(Q+1)]}{\omega_z(Q+1)}\right|^2, \tag{15}$$

where $B(\tau) = N_0\delta(t)$.

In finding $G_M(\omega_z)$, the fact that for white noise $\dot{F}_1(t, \omega_z + \omega_{zc}/P) = \dot{F}_1(t, \omega_2)$ was used.

In accordance with [2], with a low level of additive and multiplicative interference, governed by the condition: $\mu >> 1$, $EM^2/\sigma_\omega^2 >> 1$, where $\mu = 2E/N_0$ is the signal/interference ratio; E is the signal energy, the precision in the measurement of a radio signal carrier frequency in the presence of additive and multiplicative interference is determined by the expression:

$$\sigma_\omega^2 \simeq \frac{1}{T_{\text{ск}}^2 \mu}\left\{1 + \frac{\mu}{T} G_M(0)\right\}, \tag{16}$$

where $T_{\text{ск}}^2 = \dfrac{\int_{-\infty}^{\infty} t^2 |\dot{s}(t)|^2 dt}{\int_{-\infty}^{\infty} |\dot{s}(t)|^2 dt} - \dfrac{\int_{-\infty}^{\infty} t |\dot{s}(t)|^2 dt}{\int_{-\infty}^{\infty} |\dot{s}(t)|^2 dt}$ is the mean square width of the signal.

If the origin for the readout is chosen so that $\int_{-\infty}^{\infty} t|\dot{s}(t)|^2 dt = 0$,

Then
$$T_{\text{ск}}^2 = \int_{-\infty}^{\infty} t|\dot{s}(t)|^2 dt / \int_{-\infty}^{\infty} |\dot{s}(t)|^2 dt. \tag{17}$$

For a signal of the form (9):

$$T_{\text{ск}}^2 = \frac{1}{12} \cdot T^2. \tag{18}$$

Substituting (15) and (18) in (16), we obtain:

$$\sigma_\omega^2 \simeq \frac{12}{T^2}\left(\frac{1}{\mu} + WN_0\frac{T_{\text{уз}}}{T}\right), \tag{19}$$

where $T_{\text{уз}} = \dfrac{L}{V_1}$; $W = 0{,}5M^2QL$.

As can be seen from (19), the second term in the parentheses has the meaning of the signal/interference ratio for the multiplicative interference component. If $T/WN_0T_{\text{уз}} < \mu$, then the multiplicative interference has the governing influence on

the precision of the measurement of a radio signal carrier frequency as compared to the additive component.

The values of σ_ω^2 were computed using expression (19) as a function of T_{y3} for various values of μ. The signal width was taken as equal to $T = 10^{-3}$ sec, while the parameter $WN_0 = 5$ and 50. As can be seen from the graphs shown in Figure 3, the level of the multiplicative interference increases with a rise T_{y3}. This is explained by the fact that with an increase in T_{y3}, the extent of the mutual overlapping of the ultrasonic equivalents of the signal and interference in the ultrasonic light modulator aperture increases, something which leads to an increase in the power of the multiplicative interference component.

The precision of the measurement of the carrier frequency of a radio signal is shown in Figure 4 as a function of the signal width. The equivalent size of the ultrasonic light modulator aperture in this case was taken as equal to $T_{y3} = 10^{-4}$ sec while $\mu = 10$ and 10^2. Also shown in the same figure with the dashed lines are the curves for σ_ω^2 as a function of T in the absence of multiplicative interference. As follows from 4, with a decrease in the signal width, starting approximately at $T \approx 10^{-3}$ sec, the curves for σ_ω^2 as a function of T practically merge for various values of μ, something which attests to the increase in the influence of multiplicative interference on σ_ω^2 as compared to additive interference. It likewise follows from the graph that with an increase in the signal/ /interference ratio, the extent of the difference in the carrier frequency measurement precision from the potential accuracy obtained in the absence of multiplicative interference increases. This is explained by the predominance of the influence (for large values of μ) of multiplicative interference on σ_ω^2 as compared to additive interference.

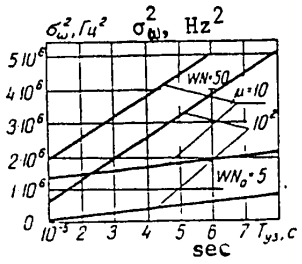

Figure 3.

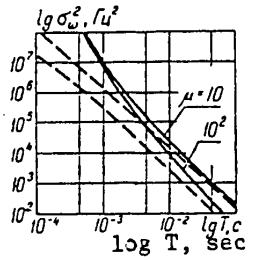

Figure 4.

BIBLIOGRAPHY

1. Kulakov S.V., "Akustoopticheskiye ustroystva spektral'nogo i korrelyatsionnogo analiza radiosignalov" ["Acoustical-Optical Devices for Radio Signal Spectral and Correlation Analysis"], Moscow, Nauka Publishers, 1978.

2. Kremer I.Ya., Vladimirov V.I., Karpukhin V.I.,"Moduliruyushchiye pomekhi i priyem radiosignalov" ["Modulating Interference and the Reception of Radio Signals"], Moscow, Sovetskoye Radio Publishers, 1972.

8225
CSO: 1860/327

UDC 621.391

COMPLEX SIGNAL RECEPTION AGAINST A BACKGROUND OF WHITE NOISE AND SPECTRALLY CONCENTRATED INTERFERENCE USING PARALLEL CHANNELS

Kiev IZVESTIYA VYSSHIKH UCHEBNYKH ZAVEDENIY: RADIOELEKTRONIKA in Russian Vol 24, No 4, Apr 81 (manuscript received 2 Jan 80, after revision 9 Jul 80) pp 63-69

[Paper by A.Ye. Ulanov]

[Text] The problem of the analysis and synthesis of a multichannel receiver for complex signals in the presence of normal fluctuating noise and spectrally concentrated interference is analyzed. It is shown that if the concentrated interference is nongaussian, the introduction of optimal nonlinear processing in the channels impacted by the interference leads to an increase in the reception noise immunity as a whole.

Protecting a complex signal receiver against a strong spectrally concentrated interference (SP) remains one of the important problems in the design of broadband communications systems.

An effective method of combatting spectrally concentrated interference is reception via parallel frequency channels, the basis for which is the principle of "whitening" the interference spectrum, proposed for the first time in [1]. The maximum signal/interference ratio which can be achieved at the output of an optimal linear combining system, as is well known [2], is equal to the sum of the signal/interference ratios in the individual frequency channels.

Actual spectrally concentrated interference has distributions of the instantaneous values which, as a rule, differ from a normal distribution. Included among them are signals from broadcasting and radio navigation stations, as well as various kinds of passive and active jamming.

It is also well known [3] that if the interference is nongaussian, the signal/ /interference ratio in the channel can be increased by means of inertialess nonlinear conversion of the input mixture.

Because of what has been presented above, the study of the question of boosting the noise immunity of the reception of complex signals via parallel channels by virtue of optimizing the nonlinear processing in each of them is an urgent issue.

The process at the input to the complex signal receiver consists of the sum:

$$X(t) = S(t) + \xi(t) + \sum_{i=1}^{l} \eta_i(t), \tag{1}$$

S(t) is a determinate, square integrable function, which determines the structure of the signal being transmitted; $\xi(t)$ is additive gaussian white noise; $\eta_i(t)$ is a function which defines the i-th spectrally concentrated interference and l is the number of the concentrated interference.

Reception is accomplished using $L >> l$ frequency channels with mutually adjacent and equal bandwidths, while each channel takes the form of the following series circuit: filter--nonlinear element--filter. It is assumed that the input and output bandpass filters have the same square-wave amplitude-frequency response.

The input process (1) is broken down by means of the input bandpass filters into individual independent frequency samples. As a result, the process at the input to the inertialless nonlinear element (BNE) of each of the channels consists of the sum of the frequency sample of the signal and the narrow band interference, which in the absence of spectrally concentrated interference in the channel is a frequency sample of just the gaussian white noise, and when it is present, takes the form of a certain nongaussian random process: an additive mixture of white noise and spectrally concentrated interference. Thus, the process at the input to an individual partial channel can be represented by the sum:

$$x_k(t) = a_k(t)\cos[\omega_{sk}t - \varphi_{sk}(t)] + R_k(t)\cos[\omega_{pk}t - \varphi_{pk}(t)] \tag{2}$$

$a_k(t)$ and $\phi_{sk}(t)$ are the envelope and phase of the frequency sample of the signal; $R_k(t)$ and $\phi_{pk}(t)$ are the envelope and phase of the resulting interference of the k-th channel ($k = \overline{1,L}$); ω_{sk} is the carrier frequency of the signal, which coincides with the center frequency of the input filter for the k-th channel, while ω_{pk} is the carrier frequency of the resulting interference, which in the general case does not match ω_{sk}.

We shall further hypothesize that the envelope of the interference in each channel has a Nakagami distribution [4]:

$$W(R) = \frac{2}{\Gamma(m)}\left(\frac{m}{\Omega}\right)^m R^{2m-1}\exp\left\{-\frac{m}{\Omega}R^2\right\}, \quad R \geqslant 0. \tag{3}$$

The Nakagami distribution is convenient in that when m = 1, it changes to a Rayleigh distribution (gaussian interference), and when m > 1, is a good

approximation of a Rice distribution, i.e., the distribution of the envelope of the sum of the gaussian narrow band process and the quasiharmonic oscillation with a constant amplitude and arbitrary phase, which is called the nonguassian interference component in the following. Distribution (1) makes it possible to analyze all of the characteristic statistical situations which arise in the individual frequency channels, from the case of interference with a probability density having maximum entropy (gaussian noise), to the case of interference with minimal entropy (harmonic interference where m = ∞).

Using the criterion of the signal/interference ratio, we shall treat the analysis and synthesis of one network section given the assumption that the desired nonlinear characteristic of the inertialless nonlinear element is approximated by the binomial:

$$f(x) = c_1(x + c_2x^3), \tag{4}$$

where c_1 and c_2 are certain coefficients.

The characteristic (4) is convenient in that on one hand, it is easily realized and is "minimally nonlinear" in the sense of generating the number of combination harmonics, and on the other hand, in accordance with [3,5], is a good approximation of the optimal nonlinear functions obtained when solving the general problem of structural synthesis for nongaussian interference, which is most frequently encountered in radio engineering practice.

By substituting (2) in (4), we will find the process which is concentrated in the first spectral band:

$$\begin{aligned} f_1(x) = c_1\Big\{\Big[1 + \frac{3}{4}c_2(a^2 + 2R^2)\Big]\, a\cos(\omega_s t - \varphi_s) + \frac{3}{4}c_2R^2a\cos\times \\ \times[(2\omega_p - \omega_s)t - 2\varphi_p + \varphi_s] + \frac{3}{4}c_2a^2R\cos[(2\omega_s - \omega_p)t - 2\varphi_s + \varphi_p] + \\ + \Big[1 + \frac{3}{4}c_2(R^2 + 2a^2)\Big]R\cos(\omega_p t - \varphi_p)\Big\}. \end{aligned} \tag{5}$$

Here and subsequently, the k subscripts are omitted.

In communications systems with angular modulation, that portion of the output frequency $f_1(x)$, which repeates the phase structure of the signal at the input, must be equated to the useful signal at the output of the inertialless nonlinear element. The first term in (5) satisfies this condition:

$$s_{out}(t) = s_{полез}(t) = c_1\Big[1 + \frac{3}{4}c_2(a^2 + 2R^2)\Big]a\cos(\omega_s t - \varphi_s). \tag{6}$$

The remainint terms of the sum (5) make a contribution to the output interference. We shall find the amount of "system gain", defined as the ratio of the average signal and interference powers at the output, normalized for the analogous value at the input [6]:

$$\Lambda = \left(\frac{Q_s}{Q_p}\right)_{\substack{\text{вых}\\ \text{out}}} \Big/ \left(\frac{Q_s}{Q_p}\right)_{\substack{\text{вх}\\ \text{in}}}. \tag{7}$$

Since the output signal amplitude is a random quantity, the output signal power must be determined as the square of the average over the entire set:

$$Q_{s\ \text{out}} = Q_{\text{вых}} = \frac{1}{2} c_1^2 a^2 \langle (a^2 + 2R^2) \frac{3}{4} c_2 + 1 \rangle^2, \tag{8}$$

The corner braces <> indicate averaging using distribution (3).

We shall define the output interference power as the difference:

$$Q_{\substack{\text{пвых}\\ \text{out}}} = \langle [f_1(x) - s_{\substack{\text{вых}\\ \text{out}}}(t)]^2 \rangle. \tag{9}$$

By carrying out the averaging and substituting (8) and (9) in (7), we obtain:

$$\Lambda = \frac{\left|1 + \frac{3}{4} c_2 (a^2 + 2\Omega)\right|^2}{1 + \frac{3}{2} c_2 (m_2 \Omega + 2a^2) + \frac{9}{16} c_2^2 (m_3 \Omega^2 + 5a^2 m_2 \Omega + 5a^4)}, \tag{10}$$

$$m_2 = 1 + \frac{1}{m}; \quad m_3 = 1 + \frac{3}{m} + \frac{2}{m^2}; \quad \Omega = \langle R^2 \rangle.$$

The problem of synthesizing the inertialless nonlinear element characteristic reduces to the determination of c2, which maximizes (10). By studying (10) for the maximum, we find:

$$c_2^0 = \frac{(q_4 - q_2) \pm \sqrt{(q_4 - q_2)^2 - (q_1 q_4 - q_2 q_3)(q_3 - q_1)}}{(q_2 q_3 - q_1 q_4)},$$

$$q_1 = \frac{3}{2}(m_2 \Omega + 2a^2); \quad q_2 = \frac{9}{16}(m_3 \Omega^2 + 5a^2 m_2 \Omega + 5a^4);$$

$$q_3 = \frac{3}{2}(a^2 + 2\Omega); \quad q_4 = \frac{9}{16}(a^2 + 2\Omega)^2.$$

The small signal case, where the signal/interference ratio at the input is $\alpha = a^2/\Omega << 1$, is of the greatest practical interest, and then:

$$c_2^0 = -\frac{4}{3}\frac{\lambda_0}{\Omega}, \tag{11}$$

$$\lambda_0 = \frac{\left(1-\frac{m_3}{4}\right)+\sqrt{\left(1-\frac{m_3}{4}\right)^2-(2m_2-m_3)\left(1-\frac{m_2}{2}\right)}}{(2m_2-m_3)}. \tag{12}$$

By substituting (12) in (10), we have:

$$\Lambda_{max} = \frac{(1-2\lambda_0)^2}{1-2\lambda_0(m_2+2\alpha)+\lambda_0^2(m_3+5m_2\alpha)}.$$

When m = 1 (gaussian interference), $\lambda_0 = 0$, $\Lambda_{max} = 1$, i.e., the nonlinear characteristic degenerates into a linear one. When m >> 1; $\lambda_0 = 1 + 0.5m$; $\Lambda_{max} = m/(1 + m\alpha) >> 1$, i.e., a considerable gain is observed because of the suppression of the nongaussian interference component.

In case the signal is masked by the nongaussian interference component and with a large signal/noise ratio at the input ($m\alpha >> 1$), $\Lambda_{max} = 1/\alpha$. This actually means that the cross-modulation product of the signal and interference, observed at a frequency of $(2\omega_p - \omega_s)$, the power of which is equal to the signal power, makes the major contribution to the output interference.

When the signal is much less than the gaussian component of the interference ($m\alpha << 1$), the gain is $\Lambda_{max} = m$. Consequently, along with the suppression of the nongaussian interference component, a decrease in the signal/noise ratio by a factor of two is also observed.

Formula (10) characterizes the gain with the assumption that the output filter passes all of the output process components without distortion.

However, if the carrier frequency of the spectrally concentrated interference, ω_p, does not coincide with the center frequency of the filter, ω_0 (frequency mismatched interference), the "generalized system gain" of [6] will be even greater by virtue of the suppression of the spectral components of the "combination" noise which falls outside the "transmittance passband" of the output filter.

In the general case, the c_2^0 inertialless nonlinear element parameters depends not only on the power parameter of the interference Ω, but on its distribution parameter m. However, this has an impact on the conversion result only for small values of m.

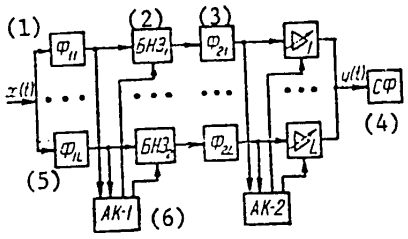

Figure 1.

Key: 1. F_{11} [input bandpass filter 1];
2. BNE_1 [inertialess nonlinear element 1];
3. F_{21} [output bandpass filter 1];
4. SF [matched filter];
5. F_{1L} [input bandpass filter L (L is the number of channels)];
6. AK-1 [channel analyzer 1].

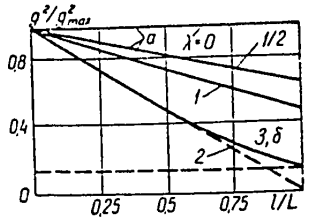

Figure 2.

The analysis and synthesis of the nonlinear elements performed here having the characteristic (4) demonstrated that with the action of nongaussian spectrally concentrated interference, the signal/interference ratio in a channel in the case of optimal nonlinear processing increases by a factor of Λ, because of the suppression of the nongaussian component of the concentrated interference, which exceeds the level of the signal and fluctuating noise. Since this result can be no further improved by means of any kind of conversion, subsequent processing reduces to the optimal linear combining of the outputs of all of the channels with weights of [2]: $c_{1k} = S_{k\ out}/Q_{pk}$, where $S_{k\ out}$ is the signal component. Q_{pk} is the interference power at the output of the k-th channel. In accordance with (11), it follows from (6) that $c_{1i} < 0$ in the channels impacted by the concentrated interference, since in these channels, $s_{i\ out} < 0$, and conversely, $c_{1i} = a_i/Q_{i\ in} > 0$ in those channels where there is no interference.

A block diagram of the adaptive multichannel nonlinear filter is depicted in Figure 1. It contains L channels, in each of which there are input F_1 and output F_2 bandpass filters, controlled by the inertialless nonlinear element and a variable gain amplifier. The analyzer of the channel (AK-1) identifies the channels impacted by the spectrally concentrated interference. In the channels where is no interference, the nonlinear circuit of the inertialless element is disconnected (linear mode). In the remaining channels, the parameters of the inertialless nonlinear element are adjusted in accordance with the adopted algorithm (the nonlinear mode). The channel analyzer (AK-2) performs the analysis of the voltage readouts at the outputs of the bandpass filters and establishes the weights with which the voltages are entered into the common sum.

We shall give the calculation of the reception noise immunity using parallel channels, taking into account the subsequent processing of the complex signal in a matched filter (SF) in two extreme cases: a) The concentrated interference is an independent sine wave which is not amplitude modulated; b) All of the interference takes the form of gaussian oscillations with rapidly changing amplitudes, and have identical dispersions while their total power is constant.

It is assumed that the signal and the signal and the noise have uniform spectral densities in the passband occupied by the complex signal.

We shall introduce the coefficient λ_k, which characterizes the degree of suppression of the "combination" noise as a function of the degree of tuning mismatch between the carrier frequency of the concentrated interference and the center frequency of the filter: $\Delta\omega_k = |\omega_{pk} - \omega_{0k}|$. In the absence of interference and in the case of its maximum frequency difference, $\lambda_k = 0$, since $\Delta\omega_k = |\omega_k - \omega_{k+1}|$. Then the maximum signal/interference ratio at the output of the optimum combining system is equal to:

$$\left(\frac{C}{\Pi}\right)_{\substack{\text{макс}\\ \text{вых}}} = q^2_{\substack{\text{макс}\\ \text{вых}}} = \sum_{k=1}^{L} \frac{2\Lambda_k}{1+\lambda_k}\left(\frac{C}{\Pi}\right)_{\substack{k,\text{вх}\\ \text{вх}}}. \tag{13}$$

It is not difficult to show that in case (a), the ratio $Q^2_{\text{вых}}$ at the output of the matched filter, in accordance with (13), is equal to:

$$q^2_{\substack{\text{макс}\\ \text{вых}}} = \left(1 - \frac{l}{L} + \frac{1}{L}\sum_{\mu=1}^{l}\frac{1}{1+\lambda_\mu}\right) 2Bq^2_{\substack{\text{вх}\\ \text{вх}}},$$

$q^2_{\text{вх}}$ is the signal/noise ratio at the receiver input; B is the complex signal base [7].

As is well known [7], the maximum signal/interference ratio is achieved in the case of ideal coherent compensation for the interference and is equal to: $q^2_{\text{max}} = 2Bq^2_{\text{вх}}$.

The curves for the ratio $q^2_{\text{вых}}/q^2_{\text{max}}$ are plotted in Figure 2 as a function of the number of impacted channels l/L for three values of $\lambda_\mu = 0$, 0.5 and 1 ($\mu = \overline{1,l}$) are the solid lines. The maximum disadvantage of adaptive nonlinear filtering as compared to ideal compensation amounts to 3 dB in all when $l/L = 1$ and $\lambda_\mu = 1$. When $\lambda_\mu = 0$, an adaptive nonlinear filter is not inferior to an ideal interference compensator.

Curves borrowed from [8] are shown in Figure 2 with the dashed lines for comparison with other well known reception methods. Straight line 1 corresponds to reception directly with the matched filter. Function 2 characterizes the noise immunity of a quasi-optimal amplitude equalizer with rejection of the spectrally concentrated interference, while curve 3 is for an adaptive linear filter. It can be seen from the graph that the gain in the reception noise immunity for the case of optimal nonlinear processing in the channels has a more substantial effect at greater values of l/L, i.e., in the case of greater saturation of the radio channel with concentrated interference, something which is quite important.

In case (b) and with optimal processing, the signal/interference ratio at the matched filter output coincides with the signal/interference ratio at the output of the linear adaptive filter, since $c^0_{2a} = 0$, $k = \overline{1,L}$ (curve 3).

It should be noted in conclusion that in a real interference situation, which is characterized by the presence of concentrated interference with different statistical properties, one can substantially boost the reception noise immunity using parallel channels by virtue of optimizing the nonlinear processing in each of the channels. One of the design solutions can be the algorithm for adaptive nonlinear filtering found in this paper, which makes it possible in a number of cases to obtain a result close to ideal compensation for spectrally concentrated interference.

BIBLIOGRAPHY

1. Kotel'nikov V.A., "Teoriya potentsial'noy pomekhoustoychivosti" ["Potential Noise Immunity Theory"], Moscow, Gosenergoizdat Publishers, 1956.

2. Andronov I.S., Fink L.M., "Peredacha diskretnykh soobshcheniy po parallel'nym kanalam" ["The Transmission of Digital Messages via Parallel Channels"], Moscow, Sovetskoye Radio Publishers, 1971.

3. Antonov O.B., "Optimal'noye obnaruzheniye signalov v negaussovykh pomekhakh. Obnaruzheniye polnost'yu izvestnogo signala" ["The Optimal Detection of Signals in Nongaussian Interference. The Detection of a Completely Known Signal"], RADIOTEKHNIKA I ELEKTRONIKA [RADIO ENGINEERING AND ELECTRONICS], 1967, 12, No 4, p 579.

4. Tikhonov V.I., "Statisticheskaya radiotekhnika" ["Statistical Radio Engineering"], Moscow, Sovetskoye Radio Publishers, Moscow, 1966.

5. Antonov O.Ye. Ponkratov V.S., "Podoptimal'noye obnaruzheniye slabykh signalov na fone amplitudno-chastotno-modulirovannykh pomekh" ["Suboptimal Detection of Weak Signals Against a Background of Amplitude and Frequency Modulated Interference"], RADIOTEKHNIKA I ELEKTRONIKA, 1975, 20, No 1, p 182.

6. Zyuko A.G., "Pomekhoustoychivost' i effektivnost' sistem svyazi" ["Noise Immunity and Efficiency of Communications Systems"], Moscow, Svyaz' Publishers, 1972.

7. Tuzov S.I., "Statisticheskaya teoriya priyema slozhnykh signalov" ["The Statistical Theory of Complex Signal Reception"], Moscow, Sovetskoye Radio Publishers, 1977.

8. Barakin L.Ye. "Pomekhoustoychivost' sistem svyazi s shumopodobnymi signalami" ["The Noise Immunity of Communications Systems with Pseudonoise Signals"], ELEKTROSVYAZ' [ELECTRICAL COMMUNICATIONS], 1979, No 1, p 42.

8225
CSO: 1860/327

UDC 621.374.55

SIGNAL PROCESSING BY MEANS OF MAGNETOSTRICTIVE TRANSDUCERS

Kiev IZVESTIYA VYSSHIKH UCHEBNYKH ZAVEDENIY: RADIOELEKTRONIKA in Russian Vol 24, No 4, Apr 81 (manuscript received 3 Jan 80) pp 98-99

[Paper by V.P. Garmash]

[Text] Functional electronics devices are widely used in modern radioelectronics [1]. Such devices include magnetostrive transducers, for which any parameter which governs the conversion efficiency is made variable along the direction of wave propagation [2].

The mechanism for generating the pulse characteristic of a pair of magnetostrictive transducers is shown in Figure 1.

A waveguide made of a material which posseses the magnetostrictive effect and is magnetically biased by virtue of an internal or external magnetization, is depicted in Figure 1a.

The input and output transducers are made in the form of single turns 1 and 2. When a current pulse (delta-pulse) is fed to transducer 1, a mechanical stress wave σ_0 appears by virtue of the magnetostriction effect, which in passing by transducer 2 excites a voltage pulse e in the latter. If the conversion effect is the same at all points in the waveguide, then assuming the position of the transducers to be variable, we obtain: $e' = e(t - x/v - y/v - L/v)$, where v is the wave velocity.

If the transducer is made in the form of a coil with a variable pitch, then the e.m.f. enclosed between planes spaded dy distance apart on a portion of a turn will be: $de = W_y e'(t - x/v - y/v)dy$, where W_y is the tangent of the slope angle of the turn (or what is the same thing, the winding density). The sign of W_y is determined by the direction of rotation of the coil. The e.m.f. from one turn of the input transducer is equal to:

$$e_1 = \int_{y_1}^{y_2} W_y e'(t - x/v - y/v)\,dy,$$

In an analogous manner, when using a complex winding at the input transducer, the expression for the total e.m.f., is:

$$e = \int_{x_1}^{x_2} \int_{y_1}^{y_2} W_x W_y e' (t - x/v - y/v)\, dy dx. \qquad (1)$$

The functions W_X and W_y are by definition real quantities. By equating expression (1) to the requisite pulse characteristic E(t), we obtain the equation for the determination of W_X and W_y.

Thus, the functions W_X and W_y realize the linear conversion of the signals e(t). Assuming that W_y is specified, we obtain the simpler function:

$$e = \int_{x_1}^{x_2} W_x e' (t - x/v)\, dx. \qquad (2)$$

The pulse-response has been recorded for transducers made in the form of single turns and placed on a waveguide made of 0J5 mm [decimal point not given in original] wire. Biasing of the transducers was used to make the form of e(t) independent of x and y.

The calculated and experimental pulse characteristics of a pair of magnetostrictive transducers with a specified distribution of terms (W_y and W_X) are shown in Figure 2. The good agreement makes it possible to conclude that there is high precision in the correspondence of the physical and mathematical models of magnetostrictive transducers with "long" coils.

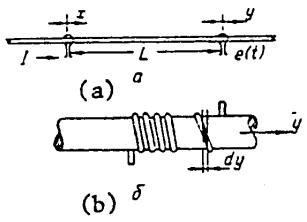

Figure 1.

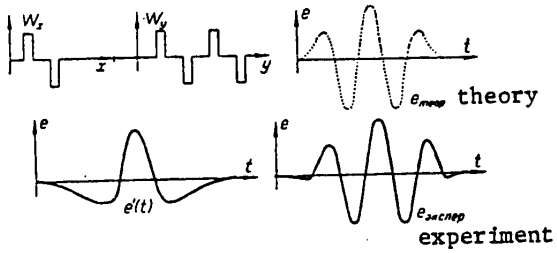

Figure 2.

BIBLIOGRAPHY

1. Soldatenkov V.A., Svistunov Yu.A., "Funktsional'noye ustroystvo - progressivnoye napravleniye mikroelektroniki" ["The Functional Device - A Progressive Trend in Microelectronics"], Moscow, Sovetskoye Radio Publishers, 1970, 11 pp.

2. Garmash V.P., "Korrektsiya impul'sa magnitostriktsionnoy linii zaderzhki, primenyayemoy v sistemakh obrabotki informatsii" ["Pulse Equalization for A Magnetostrictive Delay Line Used in Data Processing Systems"], Paper deposited in the TsNIITEIS, No. 21-83-89, 1972.

3. Zakhar'yashchev L.M., "Konstruirovaniye liniy zaderzhki" ["The Design of Delay Lines"], Moscow, Energiya Publishers, 1972, 192 pp.

8225
CSO: 1860/327

PUBLICATIONS, INCLUDING
COLLECTIONS OF ABSTRACTS

UDC 621.382

COLLECTION OF PAPERS ON SEMICONDUCTOR DEVICES AND MICROELECTRONICS

Kiev POLUPROVODNIKOVAYA TEKHNIKA I MIKROELEKTRONIKA: RESPUBLIKANSKIY MEZHVEDOMSTVENNYY SBORNIK in Russian No 33, 1981 pp 103-107

[Annotation and abstracts of papers in the collection "Semiconductor Engineering and Microwave Electronics: Republic Level Interdepartmental Collected Papers", Editor-in-Chief S.V. Svechnikov, Ukrainian SSR Academy of Sciences, Institute of Semiconductors, Izdatel'stvo "Naukova dumka"]

[Text] Papers on the components of radio electronics equipment as well as optoelectronics and microelectronics devices based on semiconductors and dielectrics are printed in the selection. The designs of new semiconductor devices, nonlinear systems and multilayer structures are described. Data are given on the properties of the various semiconductor materials and film systems. The steady-state characteristics of semiconductor devices are analyzed; the influence of various actions on the characteristics of the semiconductor devices is discussed.

The book is for scientific staff members, graduate students and engineers working in the field of semiconductor technology and microelectronics, as well as students in the advanced courses of physics and radio physics departments.

UDC 621.382.2+0.0001.5+539.293.536.5

PROPERTIES OF A SEMICONDUCTOR MATERIAL USED IN MOS INTEGRATED CIRCUIT ELECTRONICS (SILICON)

[Abstract of paper by Litovchenko, V.G.]

[Text] The characteristics of silicon material used in integrated circuit electronics are analyzed taking two factors into account: structural defects (predominantly point defects) and oxygen impurities. The specific features of the behavior of the properties of silicon plates are noted for the case of thermal action, high temperature oxidation, the influence of the dielectric layer (oxide, nitride) at the surface and a comparison of various types of defects is made with the qualitative indicators for various types of devices. Figures 10; references 60.

UDC 621.382

FIELD EFFECT MEMORY TRANSISTORS WITH ELECTRICAL UNIPOLAR DATA REWRITE

[Abstract of paper by Dobrovol'skiy, V.N., Nevyadomskiy, V.I., Ninidze, G.K. and Yarovoy, S.I.]

[Text] Field effect insulated gate memory transistors are surveyed, in which the data write and erase are accomplished by electrical unipolar voltage pulses. The various structures of such devices are described, the physical processes occurring in them are treated and the parameters are indicated. When designing memories, the use of these transistors can substantially simplify the solution of circuit design problems as compared to the case where transistors are used with different polarities for writing and erasing. Figures 8; references 68.

UDC 621.315

A STUDY OF THE METALLIZATION OF MOS STRUCTURES BY MEANS OF SECONDARY ION MASS SPECTROMETRY

[Abstract of paper by Didenko, P.I., Marchenko, R.I. and Romanova, G.F.]

[Text] The results of a study of the physical and chemical state of the Al-SiO_2-Si system using secondary ion mass spectrometry are generalized. It is shown that the nature of the energy distribution of secondary ions for the major components of the mass spectrum depends substantially on the planar inhomogeneity of the separation boundary between the metal and the dielectric. The degree of change in the structure of the dielectric film depends on the method of applying the metal electrode, something which is reflected in a change in the degree of hydration and the electrical strength of the SiO_2 layer. A structural model of the Al-SiO_2-Si system is discussed. Figures 5; references 9.

UDC 621.383.4

PARAMETERS OF AN EQUIVALENT CIRCUIT OF SANDWICH STRUCTURES BASED ON LIGHT SENSITIVE FILMS OF CADMIUM SULFOSELENIDES

[Abstract of paper by Kaganovich, E.B., Maksimenko, Yu.N. and Svechnikov, S.V.]

[Text] The resistance and reactances of an equivalent series circuit for two types of light sensitive sandwich structures are studied as a function of frequency, bias voltage and illumination. The first type of structure is fabricated using CdSe films deposited in a vacuum; the second is based on CdS powders with binders precipitated in a centrifuge.

It is shown that the real component of the impedance decreases with a rise in the frequency (200 to 2 · 10^5 Hz) from the value of the direct current resistance to a value close to the contact resistance. The existence of regions of working

parameters is established (frequency, bias voltage, illumination), in which the equivalent resistance in light exceeds its dark value. A sharp rise in the equivalent capacitance is observed as compared to the geometric values in step with increasing illumination and bias voltage at low frequencies. The conclusion is drawn that the equivalent circuits are different for the two types of structures. Figures 4; references 4.

UDC 621.315.592

MEMORY EFFECTS IN MOS STRUCTURES DUE TO THE ACTION OF RADIATION

[Abstract of paper by Kiblik, V.Ya., Lisovskiy, I.P., Litvinov, R.O. and Litovchenko, V.G.]

[Text] The characteristics (sign, density, localization) of a charge incorporated in a dielectric means of radiation, as well as the parameters (density, energy distribution) of the surface states of a Si-SiO2 separation boundary created in MOS structures by gamma and ultraviolet (UV) radiation are studied by means of the volt-faraday and the volt-ampere functions of the photoemission and contact potential difference. The analysis of the results obtained and their comparison for the cases of various kinds of radiation and irradiation conditions makes it possible to draw definite conclusions concerning the specific features of the formation and charge of electrical memory centers. Figures 7; references 13.

UDC 622.383.52

POSITIONALLY SENSITIVE PHOTOCELLS BASED ON CHALCOGENIDE TYPE CADMIUM (ZINC) COPPER-CHALCOGENIDE HETEROSTRUCTURES

[Abstract of paper by Komashchenko, V.N. and Nedostup, V.N.]

[Text] The properties of positionally sensitive biphotocells (PChF) with a transverse photoelectric effect are described, where these are fabricated based on thin film polycrystalline chalcogenide type heterostructures of cadmium (zinc) copper-chalcogenide. It is shown that the positionally sensitive photocells which were studied are characterized by a large dynamic range of the travel characteristic and high values of the slope of its linear portion, high resolving and detecting powers, as well as an operational speed, low temperature and timewise drift which are independent of the illumination of the light probe. Their fabrication technology is rather simple and economical. It allows for the fabrication of positionally sensitive photocells with a preset region and shape for the spectral sensitivity, as well as photosensitive elements of various shapes and sizes. Figures 2; tables 1; references 12.

UDC 621.382.2

ON OPTIMIZING THE BARRIER HEIGHT IN SCHOTTKY RECTIFIER DIODES

[Abstract of paper by Al'perovich, Ye.A., Bocharnikov, M.Ya., Vol'fson, E.Ye., Panichevskaya, V.I., Rozhdestvenskiy, G.F. and Strikha, V.I.]

[text] The optimum height of the Schottky potential barrier is calculated by working from a minimum of the power dissipated in Schottky barrier power diodes. The influence of the parameters of the semiconductor, the intermediate layer and the metal-semiconductor (MP) separation boundary on the optimum barrier height is analyzed. It is shown that by appropriately changing the parameters of the model for the metal-semiconductor contact, the parameters of the rectifier diodes can be adjusted. Figures 4; references 2.

UDC 621.382.2.029.64.001

THE INFLUENCE OF BORON ION DOSAGE ON THE ELECTROPHYSICAL CHARACTERISTICS OF IN-CHANNEL SAPPHIRE MOS TRANSISTORS

[Abstract of paper by Lokshin, M.M., Lyashenko, A.F. and Pelepets, P.I.]

[Text] The threshold voltage, drain-substrate breakdown voltage and drain-source leakage currents of n-channel MOS transistors on sapphire are stuided as a function of the dose of boron ions implanted in the channel region. The experimental results are compared with the calculations. Figures 3; references 10.

UDC 621.383.2

A STUDY OF THE ELECTROPHYSICAL PROPERTIES OF AN Si-SiO_2 SYSTEM OBTAINED BY THE OXIDATION OF SILICON IN WATER VAPORS

[Abstract of paper by Denisyuk, V.A., Panin, A.I., Popov, V.M. and Sukhostavets, V.M.]

[Text] The volumetric generation lifetime τ_{go}, the effective generation lifetime τ_{ge}, the rate of surface generation of minority carriers S_g, the density of structural defects with poor dielectric strength (NDP) in the oxide as well as defects with an anomalously high generation rate (AVSG) of minority carriers in Si-SiO_2 systems are studied where these systems are obtained by oxidizing silicon in water vapors in a temperature range of P = 800 - 1,000 °C. In samples obtained with T ≈ 900 °C, and stabilized FSS's [not further defined], the least generation activity level was established ($\tau_{go} \approx 1.2 \cdot 10^{-5}$ sec; $S_g \approx 10$ cm · sec^{-1}), the minimum density of defects with a poor dielectric strength was found as well as a lack of the formation of centers with an anomalously high rate of minority carrier generation. Figures 3; references 17.

UDC 621.315.592

SPECIFIC FEATURES OF THE RECOMBINATION PROPERTIES OF LARGE DIAMETER SILICON BARS, USED IN MICROELECTRONICS

[Abstract of paper by Litovchenko, N.M,, Il'chishin, V.A. and Aleksandrov, V.T.]

[Text] A comparative study is made of the recombinational properties of large and small diameter silicon bars obtained by Czochralskiy's technique which contain oxygen in a concentration of about 10^{18} cm^{-3}.

It is shown that recombination in large diameters bars is controlled by oxygen complexes which lead to a substantial difference in the lifetimes of electrons and holes. The concentration of recombination centers in such rods is substantially nonuniform over their diameter. Figures 1; references 5.

UDC 021.315.592

THE INFLUENCE OF SURFACE TREATMENT ON THE SPECTRAL DISTRIBUTION OF THE PHOTOSENSITIVITY OF $Cd_{0.2}Hd_{0.8}Te$ CRYSTALS

[Abstract of paper by Vlasenko, A.I., Matsas, Ye.P., Lyubchenko, A.B., Sal'kov, Ye.A. and Shachenko, A.V.]

[Text] The spectral characteristics of the photoconductivity of $Cd_{0.2}Hg_{0.8}Te$ crystals are studied where various surface treatments are used for the purpose of ascertaining the possibility of controlling their photosensitivity in a region of from 2 to 14 micrometers. The treatments utilized have a substantial impact on the signal amplitude and the form of the photoconductivity spectrum, where a correlation is observed between a decrease in the signal at the maximum photosensitivity and an increase in the photoconductivity in the short wave region. It is shown that the minimum surface recombination rate of S = 350 cm/sec is observed in crystals with electrically polished surfaces; all other treatments lead to a value of S and order of magnitude or more greater than this level. It is presupposed that the bulk lifetime in the surface layers of the crystals being studied is not constant and depends on the surface treatments to qualitatively explain the effects observed. Figures 1; tables 2; references 14.

UDC 621.384.3

THE CONVERSION OF INFRARED TO VISIBLE RADIATION BY ELECTROLUMINESCENT p-n STRUCTURES BASED ON GALLIUM PHOSPHIDE

[Abstract of paper by Lyubchenko, A.V., Puzin, I.B. and Sal'kov, Ye.A.]

[Text] The possibility of converting the IR radiation of low power CO_2 lasers (λ_m = 10.6 μm) to visible radiation (λ_m = 0.7 μm) by means of industrial p-n structure light diodes based on gallium phosphide is reported. The conversion effect is based on the temperature dependence of the electroluminescence intensity of the light diode structures and consists in a sharp increase in the radiation

intensity of the latter with the action of IR radiation. The effect is observed at room temperatures. Figures 4; references 14.

UDC 621.382.2

THE INFLUENCE OF GAMMA RADIATION ON THE VOLT-AMPERE CHARACTERISTICS OF SCHOTTKY DIODES BASED ON GALLIUM PHOSPHIDE EPITAXIAL STRUCTURES

[Abstract of paper by Konakova, R.V. and Faynberg, V.I.]

[Text] The results of the influence of Co^{60} gamma radiation on the volt-ampere characteristics of Au-nn$^+$-GaP Shottky barrier diodes, fabricated using nn+ gallium phosphide structures obtained by the method of liquid phase epitaxy, are given. The diode structures were breadboarded avalanche transit time diodes based on gallium phosphide. Figures 1; references 5.

UDC 621.396.963.3+621.326.001.24

ON A DYNAMIC MODEL OF MINIATURE INCANDESCENT LAMPS FOR OPTO-ELECTRONIC DEVICES

[Abstract of paper by Boguslavskiy, R.Ye. and Severinovskiy, N.S.]

[Text] Expressions are derived with precision sufficient for engineering calculations which describe the transient characteristics of miniature and subminiature incandescent lamps used at light sources in opto-electronic devices. A system of dynamic parameters is proposed for the lamps as well as a procedure for their determination by very simple experimental means. The pulsed mode excitation mode of the lamps is analyzed and basic expressions are derived for calculating it. The necessary conditions for realizing the dynamic memory storage mode in scanned matrix structures based on incandescent lamps are determined. Figures 4; references 4.

UDC 537.311

A TRANSPARENT CdO ELECTRODE FOR ELECTROLUMINESCENT FILMS

[Abstract of paper by Vlasenko, N.A., Visheva, T.P., Gergel', A.N. and Komarov, V.V.]

[Text] The influence of temperature and the duration of annealing for CdF_2 films obtained by thermal vapor deposition in a vacuum on their resistance is shown. As a result of heat treatment, CdO films can be obtained with a resistance of 50 to 100 ohms/cross-section and a transparency of about 85%. Such films were tested as transparent electrodes for ZnS:Mn electroluminescent films. A uniform contact luminescence of up to 200 cd/m^2 was obtained. The electrode sustains a current of up to 10 mA/mm^2. Figures 3; references 8.

UDC 621.383:539.1.74

A STUDY OF DEEP LEVELS IN p-TYPE SILICON USED FOR THE FABRICATION OF NUCLEAR RADIATION DETECTORS

[Abstract of paper by Voyevoda, G.P., Dubrovenko, M.Ya., Litovchenko, P.G. and Kibkalo, T.I.]

[Text] Joint studies of the structural and electrophysical properties of dislocation free silicon used for nuclear radiation detectors are presented. The parameters of the deep centers are determined in various regions with differing concentrations of small and large clusters. The different influence of A clusters and B clusters on the properties of the detectors is established. Figures 2; references 3.

UDC 621.383.539.1.74

THE INFLUENCE OF A NONUNIFORM CLUSTER DISTRIBUTION ON THE PARAMETERS OF SURFACE BARRIER DETECTORS

[Abstract of paper by Barabash, L.I., Berdnichenko, S.V., Litovchenko, P.G., Neymark, K.N., Osadchaya, N.V., Skorokhod, M.Ya. and Fal'kevich, E.S.]

[Text] The electrophysical parameters of nuclear radiation surface barrier detectors are studied as a function of the structural perfection of the raw high resistance silicon. The study of the structural defects of the dislocation-free silicon was made using X-ray diffraction topography in conjunction with decoration of the defects as well as by means of selective etching. The influence of A and B clusters on the level of the working bias of the detector and its energy resolution is demonstrated. Figures 3; references 3.

UDC 621.383:539.1.74

A MULTICOMPONENT TELESCOPE BASED ON p-Si FOR SPECTROMETRY AND IDENTIFICATION OF CHARGED PARTICLES OF INTERMEDIATE ENERGIES

[Abstract of paper by Balakin, V.D., Barabash, L.I., Berdnichenko, S.V., Kibkalo, T.I. and Kirnas, I.G.]

[Text] Experimental data on charged particle spectrometry using a semiconductor telescope are given. Completely depleted silicon detectors using especially pure and compensated silicon were used as the collection detectors in the telescope. The results obtained for the energy resolution show the advantages of this type of telescope, which are due to the increased radiation and timewise stability of the collection detectors made of p-silicon with thin insensitive input and output layers. Figures 4; references 5.

UDC 621.383:539.1.74

A STUDY OF CHARGE LOSSES IN THE NEAR-SURFACE REGION OF THE SENSITIVE LAYER OF Ge(Li)-DETECTORS

[Abstract of paper by Balakin, V.D., Petrosyan, E.Ye. and Pashchuk, N.N.]

[Text] Results of a study of the near-surface region of Ge(Li) coaxial detectors by means of a collimated beam of alpha particles are given. The correlation between the charge losses and the nature of the distribution of the electrical field intensity in the sensitive region of the detector is demonstrated. Figures 2; references 5.

8225
CSO: 1860/370

UDC 621.396.6.049.76.001

FUNDAMENTALS OF DESIGNING MICROELECTRONIC EQUIPMENT

Moscow OSNOVY KONSTRUIROVANIYA MIKROELEKTRONNOY APPARATURY in Russian 1981 (signed to press 4 Dec 80) pp 2, 302-303

[Annotation and table of contents from book "Fundamentals of Designing Microelectronic Equipment", by Aleksandr Petrovich Nenashev and Leonid Aleksandrovich Koledov, Izdatel'stvo "Radio i svyaz'", 15,000 copies, 304 pages]

[Text]

Annotation

General problems, singularities and the methodology of designing microelectronic equipment are explained. The construction of modern microelectronic components--caseless hybrid integrated circuit (IC) elements and discrete electronic components--are given. Design methods are considered for insuring temperature conditions of sections and units, protecting them from moisture and mechanical overloads, and methods and features of internal and external microelectronic equipment configuration.

The book is intended for a wide group of engineers and designers involved in developing microelectronic equipment. It may also be helpful for students at institutes of higher learning.

Table of Contents

6900
CSO: 1860/347

UDC 621.396.621.391.278

HANDBOOK ON CALCULATING NOISE-SUPPRESSION OF DIGITAL DATA TRANSMISSION SYSTEMS

Moscow RASCHET POMEKHOUSTOYCHIVOSTI SISTEM PEREDACHI DISKRETNYKH SOOBSHCHENIY in Russian 1981 (signed to press 10 Feb 81) pp 2, 230-231

[Annotation and table of contents from book "Calculation of Noise-Immunity of Digital Information Transmission Systems: A Handbook", by Valeriy Ivanovich Korzhik, Lev Matveyevich Fink and Kirill Nikolayevich Shchelkunov, Izdatel'stvo "Radio i svyaz'", 17,000 copies, 232 pages]

[Text] The structure of optimum and suboptimum decision circuits for various channels with constant and variable parameters is described in the handbook in a systematized, condensed form. The basic precise and approximate formulas are cited for calculating the probability of errors contained in monographs and articles of Soviet and foreign authors published to date. Tables of certain special functions which are widely used in calculations of noise-immunity and programs for computing them on the :Elektronika-B3-21" calculator are given. The handbook is for specialists engaged in development and utilization of means of communication.

Table of Contents

8617
CSO: 1860/304

UDC 681.325-181.48:621.3.049.77

MICROPROCESSORS

Moscow MIKROPROTSESSORY in Russian 1981 (signed to press 24 Mar 81) pp 2, 70

[Annotation and table of contents from book "Microprocessors", by Mikhail Alekseyevich Bedrekovskiy, Nikolay Serafimovich Kruchinkin and Vladimir Andreyevich Podolyan, Izdatel'stvo "Radio i svyaz'", 60,000 copies, 71 pages]

[Text] The possibilities for using microprocessors, their design structure and the features of their application in specific devices as well are demonstrated on the basis of a systematic exposition of materials reflecting the main properties and the experience of using domestic and foreign microprocessors.

For a broad circle of readers.

CONTENTS

9194
CSO: 1860/346

UDC 621.395.4

MULTICHANNEL COMMUNICATIONS SYSTEMS

Moscow SISTEMY MNOGOKANAL'NOY SVYAZI in Russian 1980
(signed to press 12 Mar 80) pp 2, 437-439

[Annotation and table of contents from book "Multichannel Communications Systems", by Aleksandr Moiseyevich Zingerenko, Natal'ya Nikolayevna Bayeva and Mikhail Serafimovich Tveretskiy, Izdatel'stvo "Svyaz'", 23,000 copies, 440 pages]

[Text] Principles for designing transmission systems are set out and fundamental questions associated with build-up of a diverse type of interference in linear channels and with the design and use of transmission systems with frequency and time division of channels.

The textbook is intended for the students of communications VUZs who are specializing in multichannel electrical communications, and it may also be useful for students in departments of automatic electrical communications, radio communications and broadcasting.

CONTENTS

COPYRIGHT: Izdatel'stvo "Svyaz'", Moskva, 1980

9194
CSO: 1860/340

UDC 681.3.07

ONE-WAY COMPUTER STORAGE

Moscow ODNOSTORONNIYE ZAPOMINAYUSHCHIYE USTROYSTVA in Russian 1981
(signed to press 20 Feb 81) pp 2, 190-191

[Annotation and table of contents from book "One-Way Storage", by Yuriy Aleksandrovich Avakh and Vladimir Konstantinovich Fatin, Izdatel'stvo "Energiya", 7000 copies, 192 pages]

[Text] New one-way storage with electrical and mechanical information exchange are examined. The operating principles and distinctive features of storage elements employing diverse physical phenomena are described, their basic characteristics are given and the most advantageous areas of application are pointed out. Methods for computing certain units and the interference level in the number-transfer block are given.

For engineering and technical workers engaged in the design of discrete computers and control devices.

CONTENTS

9194
CSO: 1860/341

UDC 621.391.63

OPTICAL COMMUNICATION CABLES

Moscow OPTICHESKIYE KABELI SVYAZI: TEORIYA I RASCHET in Russian 1981 (signed to press 23 Jan 81) pp 2, 153

[Annotation and table of contents of book "Optical Communications Cables: Theory and Design", by Nikolay Aleksandrovich Semenov, Izdatel'stvo "Radio i svyaz'", 5000 copies, 153 pages]

[Text] Optical cable (OK) is considered a constituent of an optical data transmission system which determines its fundamental properties. Physical principles of transmission of wideband signals along OKs containing lightguides (SV) of various types operating under multiple mode and single mode conditions are discussed; in some cases the concept of partial waves and beam interpretation in SV is utilized. Concepts are introduced about variable and emerging waves. A brief examination is given to typical structural circuits of communications systems using optical cable and technology for producing optical fibers.

A systematic theory of regular lightguides is evolved; modifications are derived for dispersion equations, theoretical formulas for phase and group velocities, group delay time, attenuation coefficient, power flux distribution. The corresponding program for a computer is described and results of calculation are cited. The question of optimization of the profile of the refractive index of a gradient lightguide is considered. The effect of lightguide irregularities in optical cables is discussed: flexures, microscopic bends, lightguide interconnections, interfaces with sources and receivers. Transitional attenuations between lightguides in optical cables are determined. Analysis of the passage of signals through optical cable based on chromatic and modal dispersions made it possible to determine bandpass under various operating conditions. Basic principles of optical cable design are formulated and examples of calculations of deformations in optical cable components are given.

For scientific workers specializing in development of optical cable technology, communication systems and control systems.

Table of Contents

8617
CSO: 1860/305

UDC 621.395.37

PLANNING AUTOMATIC INTERCITY TELEPHONE EXCHANGES

Moscow PROYEKTIROVANIYE AVTOMATICHESKIKH MEZHDUGORODNYKH TELEFONNYKH STANTSIY in Russian 1980 (signed to press 5 Mar 80) pp 2-3, 207-208

[Annotation, foreword (excerpts) and table of contents from book "Planning Automatic Intercity Telephone Exchanges", by Fanya Bentsionovna Bakaleyshchik, Izdatel'stvo "Svyaz'", 10,000 copies, 208 pages]

[Text]

Annotation

This book presents the basics of planning automatic intercity telephone exchanges using type AMTS-3, AMTS-4, ARM-20, AMTS KE equipment and automatic switching unit.

The book is intended for engineering and technical workers involved in planning and operating automatic intercity telephone exchanges.

Foreword

The creation of a nationwide automatically switched telephone network involves the construction of automatic intercity telephone exchanges (AITE) and automatic switching units (ASU). In the process of being developed, modern technical automatic switching facilities are reaching higher quality levels; telephone exchanges with new capabilities and new switching and control principles are being created.

The present book is the first attempt at a systematic exposition of the basics of planning AITE and ASU of various types considering their interaction in a network. As new equipment is developed and assimilated, it will become possible to introduce appropriate modifications and improvements to planning methodology.

Table of Contents

6900
CSO: 1860/344

UDC 621.397.611:621.397.65

RADIO AND TELEVISION TRANSMITTING STATION EQUIPMENT

Moscow OBORUDOVANIYE RADIOTELEVIZIONNYKH PEREDAYUSHCHIKH STANTSIY
in Russian 1981 (signed to press 15 Oct 80) pp 2, 238-239

[Annotation and table of contents from book "Radio and Television Transmitting Station Equipment", by Viktor Konstantinovich Ivanov, Izdatel'stvo "Radio i svyaz'", 14,000 copies, 240 pages]

[Text] Annotation

Questions of transmitting network construction are examined, general principles of constructing various types of stations are given, the most important pieces of equipment are examined in detail, and some types of television relays and low-power transmitters are described. Separate chapters are devoted to measurement and monitoring equipment and measurement methods.

The book is intended for technical communication training school students in the course on specialty No. 0706; it may be helpful for a wide group of technical workers who operate the equipment in question.

Table of Contents

6900
CSO: 1860/345

UDC 621.314.58(088.8)

SOLID MAGNETIC VOLTAGE CONVERTERS FOR RADIO POWER SUPPLY

Moscow MAGNITNO-TRANZISTORNYYE PREOBRAZOVATELI NAPRYAZHENIYA DLYA PITANIYA REA in Russian 1981 (signed to press 2 Oct 80) pp 2, 97

[Annotation and table of contents from book "Magnetic Transistor Converters of Voltage for Powering Radioelectronic Equipment", by Boris Aleksandrovich Glebov, Izdatel'stvo "Radio i svyaz'", 8000 copies, 97 pages]

[Text] Variable voltage converters (inverters) are examined, a typical feature of which is the use of a single magnetic reactor with any number of galvanically separated output channels. Circuits are classified by the principle of adjustment and control of energy on the load. The operation of some modifications of variable inverter circuits is analyzed. Methods are given for calculating the basic characteristics of these circuits and defining component parameters. For technical engineering workers engaged in development and operation of secondary radio power supply sources.

Table of Contents

8617
CSO: 1860/307

UDC 621.397.6

TELEVISION DATA DISPLAY DEVICES

Moscow TELEVIZIONNYYE USTROYSTVA OTOBRAZHENIYA INFORMATSII in Russian 1981 (signed to press 4 Dec 80) pp 2, 198-199

[Annotation and table of contents from book "Television Data Display Devices", by Il'ya Naumovich Guglin, Izdatel'stvo "Radio i svyaz'", 7000 copies, 200 pages]

[Text] The author examines physical principles of the formation of TV signals of data display by digital methods, classification of TV data display devices, structural principles of modern alphanumeric displays, special structural characteristics of data display devices used in ASU [automatic control systems] and subscribers' information complexes, including the "Teletext" system. Much attention is given to the problems of designing microprocessors and specialized data display devices.

This book is intended for engineers and technicians specializing in the area of data display systems in television, computers, telesignalization, and other areas.

Contents

10,233
CSO: 1860/342

UDC 621.382+621.396.6

THEORY OF SOLID STATE ELECTRONICS AND INTEGRATED CIRCUITS

Moscow FIZICHESKIYE OSNOVY KONSTRUIROVANIYA, TEKHNOLOGII REA I MIKROELEKTRONIKI in Russian 1981 (signed to press 5 Mar 81) pp 2, 247-248

[Annotation and table of contents from book "Physical Principles of Design and Technology of Radio Electronics Equipment and Microelectronics", by Aleksandr Andreyevich Shternov, Izdatel'stvo "Radio i svyaz'", 25,000 copies, 248 pages]

[Text] The foundations of processes determining the operating principles of radio and microelectronic equipment are set forth. The structure of solids, their electrophysical properties are examined in detail; contact, surface, acoustic and optical phenomena are discussed; phase conversions and thin film effects are investigated.

The handbook for a course in "physical foundations of design and technology of radio electronics and microelectronics" is for students majoring in design and production of radio equipment. It will be useful to students in related majors and to a broad range of specialists in the radio industry.

Table of Contents

8617
CSO: 1860/303

UDC 621.396.96.001(07)

THEORY AND TECHNIQUES OF RADAR DATA PROCESSING AGAINST THE BACKGROUND OF INTERFERENCE

Moscow TEORIYA I TEKHNIKA OBRABOTKI RADIOLOKATSIONNOY INFORMATSII NA FONE POMEKH in Russian 1981 (signed to press 20 Apr 81) pp 2-3, 410-416

[Annotation, foreword and table of contents from book "Theory and Techniques of Radar Data Processing Against the Background of Interference", by Yakov Davidovich Shirman and Vladimir Nikolayevich Manzhos, "Radio i svyaz'", 10,000 copies, 416 pages]

[Text] The authors generalized the problems of the optimization of multichannel and single-channel detection, measurement and resolution of radar signals.

Main attention is given to the principles of synthesis and problems of technical realization of various analog and digital detectors and meters of signal parameters against the background of correlated nonsteady-state interferences, problems of the adaptation to the conditions of a priori ambiguity, etc. A large number of illustrative examples are given.

The book is intended for specialists engaged in the theory, design and operation of radioelectronic facilities and systems.

Foreword

The rapid development of radioelectronics, and the theory and techniques of processing radar information in particular, makes it difficult to generalize various publications in this area. However, there is an urgent need in generalizing publications covering the present state of the theory and the prospects for the realization of its conclusions.

Therefore, the generalization of the "established" and new problems of processing radar information against the background of interferences from a single sufficiently general, methodological position is an urgent but difficult problem. For example, the improvement of the element base broadened the possibilities of multichannel reception. Signals and interference are described by sets of time functions, or by functions of time and coordinates. Space-time processing of signals against the background of interference ensuring its effective suppression (not only in radar) becomes the subject of optimization. Generalization of new problems of such processing is a substantial part of the goal stated above.

This book is an attempt to solve this problem to some degree. It is based on courses of lectures on the radar theory: for engineers improving their skills; for graduate students and candidates preparing for postgraduate examinations. Special attention is given to problems which are not always clearly and fully explained in published sources: theory of primary space-time processing of radar information against the background of correlated interferences with provision not only for the accumulation of useful signals but also for compensating interfering signals; theory of measuring of signal parameters changing and not changing in time against the background of interference in the process of primary and secondary processing; adaptation theory; adaptive antennas and moving target selection systems; new methods of coherent processing of simple and complex space-time signals -- digital, optical, and spin methods.

Much attention is given to the compactness, uniformity and simplicity of presentation of relatively complex theoretical material. The book reflects many years of teaching experience and personal investigations of the authors in this area. Many examples are given. The book will be useful not only to engineers and graduate students, but also to undergraduate students of vuzes. Materials which until now could be used by a narrow circle of researchers have now become accessible to many others.

The authors express their gratitude to V. Ye. Dulevich, D. I. Lekhovitskiy and M. B. Sverdlik for their useful comments.

Contents

10,233
CSO: 1860/343

UDC 621.396.2

WIDEBAND ANALOG COMMUNICATION SYSTEMS WITH COMPLEX SIGNALS

Moscow SHIROKOPOLOSNYYE ANALOGOVYYE SISTEMY SVYAZI SO SLOZHNYMI SIGNALAMI in Russian 1981 (signed to press 19 Dec 80) pp 2, 153

[Annotation and table of contents of book "Wideband analog systems of communication with complex signals", by Petr Fedorovich Polyakov, Izdatel'stvo "Radio i svyaz", 2,250 copies, 153 pages]

[Text] Questions of utilization of complex signals in analog systems of transmission of continuous messages along radio channels with continuous and randomly alternating parameters, additive functional and concentrated noise are set forth. Methods are considered for formulating complex analog signals; algorithms are determined for optimum (adaptive) and quasi-optimum reception for single and multiple beam channels of radio communications and their corresponding receivers. Their noise-immunity is analyzed. Recommendations are made for selecting the basis of a complex signal as a function of the noise affecting it.

For scientific workers engaged in research and development on communications systems.

Table of Contents

8617
CSO: 1860/306

CRYOELECTRONIC RECEIVING MODULES USING HYBRID INFRARED BAND CHARGE COUPLED DEVICES

Moscow POLUPROVODNIKI, SVERKHPROVODNIKI I PARAELEKTRIKI V KRIOELEKTRONIKE in Russian 1979 pp 350-364

[Section 6.8 and relevant bibliography from the book by V.N. Alfeyev: "Semiconductors, Superconductors and Paraelectrics in Cryoelectronics", Izdatel'stvo "Sovetskoye radio"]

[Text] 6.8. Cryoelectronic Receiving Modules Using Hybrid IR CCD's.

As was shown in §6.6, cryoelectronic modules have been used to an ever greater extent in recent years for remote sensing in the IR band in various fields of science and engineering. This has been greatly stimulated by the development of thermal imagers in medicine for the determination of the heat picture of the human body for the purpose of early diagnosis of numerous illnesses at small distances from the object to the receiver, as well as the development of scanners for the study of the earth's natural resources in meteorological, geological and other research at great distances from the radiation source [17]. All of this work would be impossible without the synthesis of new narrow band semiconductor materials, the width of the forbidden band in which corresponds to the low energy of the quanta in the various regions of the IR band, without the creation of new methods of fabricating diode structures which have a high detection capability, without the development of low noise, small signal amplification techniques and without the successes of cryogenic engineering and methods of scanning within a specific field of view. Despite the design of various types of charge coupled devices during 1970 - 1976 [33, 34, 54], mechanical scanning receivers with a single cryoelectronic IR receiver and an autonomous cryogenic installation for continuously maintaining the requisite cooling level have become the most widespread in IR receiving systems operating at long ranges. If moving images are received, the scanning is accomplished in one plane using the well-known configuration adopted for thermal imagers (Figure 6.13).

The received signal of one "point" of an image in the IR band passes through the scanning mirror (1) (or rotating prism) to the input of the optical IR mirror system (2) and is focused on the sensitive area of the IR receiving element (3), which is coupled to the low noise preamplifier (4) located in cryostat (5). Unit (6) is coupled to a photographic recorder which has a light source, the beam of which travels over photographic film synchronously with the motion of mirror (1), recording the intensity of each point of the IR image in a horizontal line.

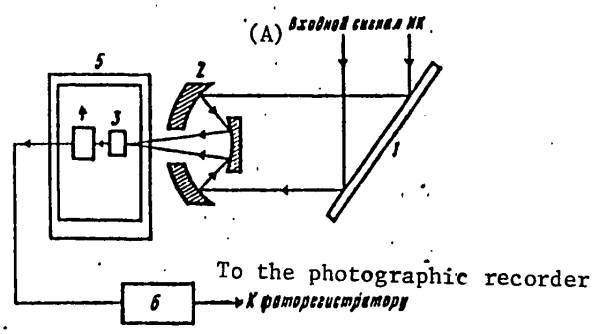

Figure 6.13. Electromechanical cryoelectronic scanning receiver for the infrared band.

Key: A. Input IR signal.

Multiple element IR receivers which operate in various portions of the IR spectrum are used to improve the resolution of such systems and provide for pattern recognition. The type S-192 multichannel cryoelectronic scanning receiver, installed in the "Skylab" (U.S.), with 12 channels in the visible, near and middle IR regions (to 2.5 μm) and with a 13th channel for 10.8 - 12.5 μm [12] has extremely good parameters. This device is made using a single $Cd_xHg_{1-x}Te$ semiconductor material and is cooled to a temperature of 90 °K.

The fundamental drawback to all mechanical IR scanning receivers is the peripheral distortion of the diameter of the circle of confusion which falls on the receiving element, with a deviation from the main optical axis of just a slight viewing angle, as well as the impossibility of controlling the scan in a wide range, the necessity of having special electronic circuitry for the utilization of multiple element receivers and mechanical devices with an electric motor. The use of electronic scanning with CCD's makes it possible to eliminate the deficiencies enumerated above and enjoy the new functional capabilities in them. For this reason, the development and study of CCD's and IR band receivers using CCD's have become a promising field in recent years in which numerous researchers are at work [33-36]. One of the major problems confronting designers consists in retaining the same ultimate sensitivity in an electronically scanned system as in a single receiver with a stationary reflector and making use of the advantages which deep cooling yields so as to improve the noise and amplification properties of CCD's.

The scanning task is facilitated in thermal imaging receivers in that the images received only by one line of IR receiving elements, the number of which for a specified resolution (size of the sensitive receiving area) determines the aspect angle when viewing the terrain. For this reason, it is expedient to construct the receiver in two ways: the element by element connection of each of the receivers of the infrared strip, which is fabricated from a narrow band material, to the input cells of a silicon CCD shift register, which performs the function of series-parallel conversion and information compaction; or by setting up a matrix of IR linear strips, each of which is connected element by element to a CCD register, which plays the part of an adder for charge storage, where the output of each CCD adder is connected to the corresponding cell of the output shift register.

When both of these methods are used, it is necessary to insert a differential amplifier at the output of the CCD register, where an additional CCD register is simultaneously connected to the amplifier to suppress the clock noise. A schematic cryostat contained hybrid infrared CCD with a three cycle supply (Φ_1, Φ_2, Φ_3) is shown in Figure 6.14.

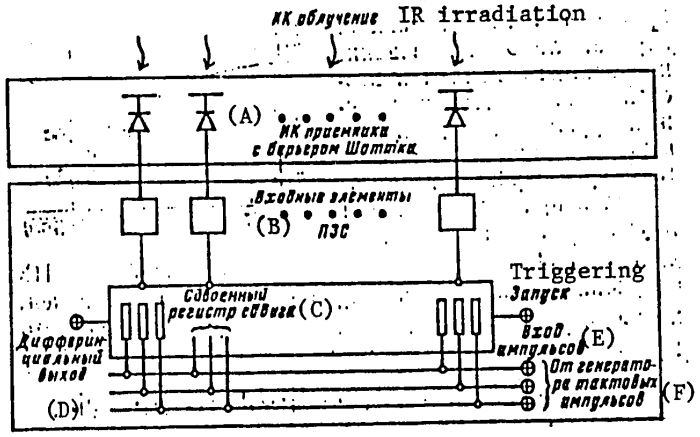

Figure 6.14. Schematic of a hybrid cryoelectronic IR charge-coupled device.

Key: A. Infrared Schottky barrier receivers;
B. CCD input elements;
C. Dual shift register;
D. Differential output;
E. Pulse input;
F. From the clock pulse generator.

An entire series of complex problems which derive from the following main requirements must be solved in the design of hybrid CCD's which operate in various portions of the infrared band: the values of the spectral volt-watt sensitivity of infrared CCD's should approximately correspond to these values for individual IR receiving elements; the internal noise level and the value of the detection capability D* of an IR band hybrid CCD should be of the same order of magnitude as in individual IR elements, and in this case, the clock noise must be suppressed to a level at which it does not degrade the signal/noise ratio at the output of the linear channel with the CCD's; the speed and passband of the device should on the whole assure its operation in image receivers; the size of the sensitive receiving area of the IR elements and the step in the chip of the linear strip of IR receivers should govern the size of the step in the CCD shift register; the amount of heat due to heat influx via the connecting conductors, which exit the cryostat housing of the hybrid IR CCD, and the amount of heat liberated by the elements of the device should not exceed $(0.2\text{--}0.3)Q_\Sigma$, where Q_Σ is the total heat influxes in the cryostat, and the uniformity of the parameters should be high. To resolve these problems, it is first of all necessary to develop techniques for the design of the input and output circuits in hybrid CCD's. We shall consider a few input circuits which are necessary for matching the output of a cooled IR receiving

element to the input to the first cell of a register using silicon MOS charge coupled devices. *Hybrid CCD's with direct charge injection.* The simplest input device is one consisting of a p-n junction and controlling insulated gates, which provide for either for the creation of a potential well for the storage of the injected charge or the formation of a conducting inversion channel for the overflow of the injected charge into the first potential well of the CCD register. This is also preserved when two or three gates are used.

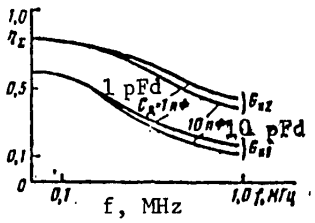

Figure 6.15. The coefficient of charge injection in infrared band hybrid CCD's as a function of frequency.

One can write $I_Д = I_1 + I_{CCD}$ for the current of the IR receiving element when exposed to IR irradiation and the coefficient of injection from the IR element into the potential well of the CCD is equal to:

$$\eta_\Sigma = I_{ПЗС}/I_Д = g_m R_Д/[R_Д(C_{OS} + C_Д) + (1 + g_m R_Д)].$$

The calculated curve for the injection coefficient η_Σ is shown in Figure 6.15 as a function of frequency for various values of g_m [micromhos] and the capacitance of the input p-n junction $C_Д$, if the IR element (PbSnTe) has $R_Д$ (V = 0), A ≈ 0.7 ohms · cm^2 and $C_Д$ (50 mv) ≈ 45 pFd. As can be seen from the figure, at low frequencies the conductance of the input junction exerts the main influence on the value of η_Σ, and at relatively high frequencies (more than 100 to 150 KHz), the capacitance of the input junction begins to have an impact.

The coefficient η_Σ depends on a number of factors: on the ratio of the voltages at the gates and the p-n junction, on the degree of overlap of the p-n junction by the input gate and the ratio of their capacitances as well as on the mutual positioning of the input gate electrodes and the first electrode of the CCD. In turn, depending on the operational mode of the CCD, the circuit configuration of the input gate or that for the formation of the MOS capacitor, or for the formation of the conducting channel connecting the p-n junction to the first potential well in the cell, the virtual drain of the MOS transistor, can have an influence on the coefficient η_Σ. When a supplemental floating low capacitance diffusion region is used in the input device to reduce the level of input noise, the injection coefficient η_Σ can be slightly reduced.

Stickle et al. [35] analyzed the signal/noise ratio for infrared band hybrid CCD's with direct charge injection, which utilize a summing with delay operation. For a hybrid IR system with a matrix of nine photodiodes based on (HgCdTe) at (λ = 12 μm) under standard conditions (T_b = 300 °K, a field of view angle of 90°), a signal/noise ratio on the order of 500 was obtained for a photon flux of 3 · 10^{17}, the dynamic range was 300 and the increase in the useful signal because of the noise was equivalent to a temperature range of 0.1 °K.

If only the low frequency range is considered and the influence of modulation is neglected, then the equivalent circuit of a hybrid CCD for the case of direct injection will contain the parallel connected conductance and capacitance of the photodiode and the overall conductance and capacitance of the CCD input. The light sensitivity of the photodiode in the idealized case is determined from the expression:

$$I_д = I_s(\exp qV/kT - 1) + I_ф, \tag{6.41}$$

where I_S is the inverse diode saturation current, $I_Ф$ is the photogeneration current, where $I_ф = ηqΦ_bA$ and $Φ_b$ is the photon flux.

As is well known, the quantity I_S depends on the resistance of the photodiode R_0 as follows for the case of zero bias:

$$I_s = kT/qR_0 \tag{6.42}$$

The signal current distribution for a bias voltage across the diode V = 0, will correspond to the expression:

$$I_{CCD} = I_{пзс} = I_ф/(1 + g_m^{-1}R_0^{-1}), \tag{6.43}$$

since the overall current is

$$I_г = I_ф(1/R_0 + g_m). \tag{6.44}$$

The slope of the CCD input in the small signal case is expressed by the ratio for the conductance g_m:

$$g_m = \frac{Z}{L}\mu C_{окс}\left(\frac{kT}{q}\right)\left\{\left[1 + \frac{2I_{пзс}}{\mu C_{ок}Z/L}\left(\frac{q}{kT}\right)^2\right]^{1/2} - 1\right\}, \tag{6.45}$$

where Z/L is the ratio of the geometric dimensions of the input gate, μ is the minority carrier mobility, $C_{ОКС}$ is the capacitance of the oxide per unit area.

The signal injection efficiency is expressed by the ratio I_{CCD}/I_{Φ} and it is therefore desirable that this quantity be as close as possible to unity. This means that the entire current generated by the photon flux in the photodiode goes to the CCD register. It follows from expression (6.43) that the product $g_m R_0$ should be large for large values of the injection efficiency, although the dependence of g_m on I_{CCD}, as can be seen from (6.43), complicates the picture.

We shall analyze the so-called subthreshold mode, which is defined by the relationship:

$$I_{\text{пзс}} \ll \frac{Z \mu C_{\text{окс}}}{2L} \left(\frac{kT}{q}\right)^2. \tag{6.46}$$

For a typical input circuit of a silicon CCD, having

$Z/L = 4$, $\mu = 700$ cm$^2 \cdot$ V$^{-1} \cdot$ sec^{-1}, $C_{\text{Д}} = 3 \cdot 10^{-8}$ F/cm^2 and $T = 300$ °K,

The ultimate current is approximately 30 nA.

If the function

$$\sqrt{1 + \frac{2I_{\text{пзс}}}{\mu C_{\text{окс}} Z/L} \left(\frac{q}{kT}\right)^2}$$

is represented as a function of the small parameter $\sqrt{1+x}$ and is expanded in a Taylor's series, by limiting ourselves to the zero and first term of $f(x) = 1 + (1/2)x + \ldots$, then in the chosen mode, the expression for g_m in formula (6.45) reduces to:

$$g_m = qI_{CCD}/kT \tag{6.47}$$

$$g_m = qI_{\text{пзс}}/kT.$$

Then expression (6.44) will assume the form $I_{CCD} = I_{\Phi} + kT/qR_0$. It follows from this that the condition $I_{\Phi} >> I_S$ provides for 100 percent signal charge injection. For photovoltaic receiving IR elements, this likewise means a condition of limitation on the sensitivity by the external background (BLIP). The background limitation condition, as was demonstrated earlier, is extremely important, since this means 100 percent signal charge injection, high linearity of the light response between I_{CCD} and Φ_b as well as good uniformity of the channel, which does not depend on the value of R_0. The total noise voltage of the photodiode is:

$$e^2_{\text{д}} = \left(\frac{4kT}{R_0} + 2qI_{\Phi}\right) R^2_0, \tag{6.48}$$

where the first term of the expression in parentheses represents the diode Johnson noise, while the second term represents the induced photon shot noise

current. The CCD noise voltage, on the other hand, is expressed as follows:

$$e^2_{CCD} = e^2_{пзс} = 8kT/(3g_m) + e^2_{1/f}, \quad (6.49)$$

where the first term is the Johnson noise of the strongly inverted channel region and the second is 1/f type noise.

The value of the specific detection capability D* for a hybrid IR band CCD can be defined as:

$$D^*_{CCD} = D^*_{пзс} = D^*_{\lambda}\sqrt{F}, \quad (6.50)$$

where the noise factor F is defined as the ratio of the total noise power to the photodiode noise power. When substituting, F is expressed as:

$$F = 1 + \frac{(8/3)\,kT\,(2L/\mu C_0 Z I_\phi)^{1/2} + e^2_{1/f}}{R^2_0\,(4kT/R_0 + 2qI_\phi)}. \quad (6.51)$$

In the experiments of Sato Iwasa and Vita with a single HgCdTe photodiode in a range of wavelengths close to 5 μm, as well as those of Stickle, Alfeyev, Bovina, Krev, Legezo, Stafeyev, Shamanayev, Nelson, et al. with multielement HgCdTe photodiodes in strips in a range of wavelengths of 8 to 12 μm, the possibility of introducing electrical charges from photovoltaic receiving elements based on narrow band solid ternary solutions, into a silicon CCD shift register was demonstrated for the first time, where these elements were connected in the circuit of a far infrared band hybrid CCD [36, 37]. With the optimum selection of the technology for a wavelength of $\lambda \simeq 5$ μm [36], such a photovoltaic cell has a high impedance, since its equivalent circuit (at $\lambda = 5$ μm) consists of a resistance of $\geq 10^6$ ohms and a capacitance on the order of a few picofarads, connected in parallel, and dissipates a low power: < 1 microwatt.

A direct injection experiment at a wavelength of 5 μm was performed with a single photodiode based on p-n junction, fabricated on a p-type substrate by means of directly connecting the p-region of the photodiode to the p-region of a CCD with a surface channel, and the n-region of the photodiode to the n-region of the diffusion source of the CCD. The parameters of this photodiode are given in Table 6.2.

A two-phase supply for the carry electrodes was used in the CCD registers as well as an input read gate made of Al, which was connected to phase Φ_1 of the clock supply at a frequency of 500 KHz. A bias voltage of approximately -1 V was

fed to the electrodes made of polysilicon in order to provide for an input current of 0.2 μA for the purpose of compensating the photoelectric current of the photovoltaic receiving cell generated by the background and thereby providing for the operation of this element at zero bias.

TABLE 6.2

The Parameters of a Photovoltaic Cell Based on HgCdTe for the Central Infrared Band

Parameter, Measurement Units	
D* for an aspect angle of 180° and a background temperature of 300 °K, cm · $Hz^{1/2}/W$	$1.6 \cdot 10^{11}$
D* for an aspect angle of 180° and a background temperature of 77 °K, cm · $Hz^{1/2}/W$	$2.5 \cdot 10^{12}$
The area $A_д$, cm^2	$1.82 \cdot 10^{-4}$
Resistance R_0 at 77 °K, MOhm	20
Maximum sensitivity wavelength, μm	4.4
Longwave sensitivity limit, μm	4.76
Zero bias diode current, μA	0.2
Quantum efficiency η	0.74
The product $R_0A_д$ at T = 77 °K, ohms · cm^2	3,640

Black body radiation at T = 500 °K was modulated by a mechanical modulator at a frequency of 723 Hz. The modulated signal was processed by selective and broadband amplifiers, and was measured by means of spectrum analyzer in a passband of 10 Hz. The spectral noise density at the CCD output amounted to 6 $\mu V/Hz^{1/2}$ at 723 Hz. In the experiment of [36], the HgCdTe photovoltaic cell operated at a typical signal/noise ratio value of 600. In the case of the direct connection of the photodiode to the CCD input, the signal/noise ratio at the CCD output proved to be 600 ± 100. These values correspond to the value of the detection capability D* for a single photodiode, corresponding to $1.6 \cdot 10^{11}$ cm · $Hz^{1/2} \cdot W^{-1}$. The signal and noise are generated only by the HgCdTe photodiode and the output of the hybrid circuit with the CCD, something which is clearly demonstrated by the oscilloscope traces in [36]. The noise factor of the given hybrid circuit, computed from formula (6.39), amounted to F = 1.0 for the following data, which were obtained experimentally: R_0 = 20 MOhm, I_ϕ = 0.2 μA, T = 77 °K, $e_{1/f} = 18/f$ $[\mu V^2/\sqrt{Hz}]$ and the CCD parameters given above.

Thus, for the case of direct charge injection in the CCD, the value of the detection capability of the string of infrared band photodiodes, connected element by element to the input of a multiple input shift register using a SI-CCD in a

hybrid circuit configuration, can be no worse than the value of D* of a single photodiode. In this case, each photodiode cell based on HgCdTe can dissipate a power on the order of I^2R_0 = 0.8 μW, something which is an insignificant amount as compared to the power dissipated by photoresistive type receiving IR elements.

A circuit is given in paper [37] for an experimental unit to study the reception of the emission of a CO_2 laser by a far IR band hybrid CCD using light receiving cells made of $Hg_{0.8}Cd_{0.2}Te$. In this unit, the laser radiation passes through a mechanical modulator to a photodiode string made of HgCdTe cells, each of which is connected either directly or through a multichannel amplifier to the p-n junctions of the input cells of the multiple input silicon CCD shift registers with three phase supply and molybdenum transport electrodes. The hybrid CCD is placed in a cryostat with liquid nitrogen, having an input window made of clear coated Ge. The CCD electrodes and the output stage designed around MOS transistors are driven from a clock pulse generator at a working frequency of 250 KHz, located outside the cryostat.

The signal from the CCD is fed to a differential amplifier to suppress the "clock" interference and through a matching device to a dual trace oscilloscope. The signal from the CCD is fed to the input for one trace while the signal from an additional photodiode is fed to the other, where this diode registers the modulated radiation directly from the CO_2 laser. An attenuator which attenuates the laser power down to the requisite values in placed between the laser and the mechanical modulator operating at a frequency of 60 Hz.

The silicon CCD is made in the form of 16-input MOS type structure with a step of 100 μm having a common control gate for all the inputs and diffusion p-n junctions which are not overlapped by the control gate, for the injection of charge carriers from the photodiodes into the potential wells under every third transport electrode. When a photoresistive linear strip for the IR band is used, special matching circuitry is employed. The charge transfer loss factor in a CCD shift register cooled down to T = 77°K was reduced by a factor of 10 as compared to the value at T = = 300 °K. The signals from the receiving elements can also be fed to the gates.

The dimensions of the IR radiation sensitive areas are 100 x 100 μm. The p-n junctions were produced by mercury diffusion and the ohmic contacts were made using indium. The doping depth of the p-n junction was 15 to 20 μm and the photoresistor thickness was 20 to 30 μm. The volt-watt sensitivity was higher than 10^3 V/W. The photoreceiving elements are arranged on a substrate of leuco-sapphire. Measurements of the characteristics which were made ahead of the input of the CCD and following the CCD demonstrated the total identity of the modulated signals and the small signal losses when the signal received from the CO_2 laser passes through the hybrid IR band CCD.

No nonlinearity was detected in the output signal when the laser signal power was varied by more than 40 dB. The output signal level with an increase in the temperature of the silicon CCD register up to T = 300 °K and the IR element temperature kept at T = 77 °K was reduced by a factor of two to three. Similar results were also obtained when PbSnTe elements were used.

[illegible] demonstrates the complete capability of designing [illegible] based on HgCdTe and PbSnTe which cover various regions of the [illegible] to the far infrared. The creation of matrix far IR band CCD's [illegible] 77 °K with heterodiodes becomes possible when an epitaxial [illegible] solution of a ternary compound is obtained directly on the surface [illegible] semiconductor substrate chip.

[illegible] is used between the linear strip of photodetectors and the CCD [illegible] register in IR band hybrid direct injection CCD's. Various components can [illegible] part of the buffer stage - from an MOS transistor up to one or more independent amplifiers on the same chip. This is a variant, the merits of which consist in the simplicity and ease of integration. We shall consider two types of indirect injection devices, in one of which photoconductive thin films are used while pyroelectric receiving films are used in the other [33].

Hybrid IR band CCD's based on photoconductive films. Any photoconductive film which can be successfully deposited on silicon dioxide without creating fast states (or traps) at the separation boundary between the silicon and the silicon dioxide can be used in devices of this kind. The role of the photoconductive film consists in acting directly on the inversion channel of the input MOS transistor which is connected to the CCD element. The degree of inversion in turn determines the rate of charge transport in the CCD. The number of input MOS transistors which can be fabricated on a single chip with a CCD shift register corresponds to the number of photoconductive film receiving elements. The advantage of this device consists in the fact that the photoconductive film can be precipitated in various ways following the formation of the MOS charge coupled device on the oxide or on the Si to create hetero-CCD's.

The operation of this device is described by the following sequence of operations for the case of a photoresistor at the gate:

--A voltage is fed to the film bias electrode. It should be sufficiently high to produce the inversion of semiconductor conductivity at the oxide--semiconductor separation boundary underneath the photosensitive elements;

--Voltage is supplied to the control electrode so as to provide the requisite level of resistance which is inserted in series with the photoconducting gate;

--The bias voltage at the photoconducting gate is set somewhat higher than the threshold voltage level for this gate. This leads to maximum charge transport in the absence of an optical input signal and prevents the blurring of the image;

--The incident IR band photons cause a reduction in the resistance of the photoconductive films. As a result, the voltage drop across each photoconductive film proves to be inversely proportional to the local density of incident photons;

--The charge transported in the CCD now becomes a function of the intensity of the IR illumination of the photoconductive film. The nature of the transient phenomena in the device in the nonsteady-state illumination mode is governed by how rapidly the capacitance of the photoconductive gate is discharged through the bias resistor.

A device of this type, in being a hybrid indirect injection device, makes it possible to design a straightforward and technologically simple linear or matrix IR image reception system using CCD's. Another structural configuration is also possible for the hybrid CCD's, in which the photoresistive IR receiving elements are made in the form of linear strips of photoresistors on a monocrystal of a narrow band material, for example, HgCdTe or PbSnTe, which is secured to a common passive substrate with a multiple input CCD shift register. In such a device design, which is used primarily in linear video receivers, the signal input elements for the CCD can have an internal gain or be made just as in the case where photoconductive films are used, only a group layout is necessary for the contact metal films from the monocrystal of the IR photoresistors to the CCD chip, without forming individual contact areas which take up considerable space, and possibly, the connecting of the photoresistors to the input CCD diodes.

*Hybrid indirect injection CCD's based on film pyroelectric receivers**. Pyroelectric materials are used because of the fact that IR radiation can be registered due to the strong temperature dependence off the polarization (a review of pyroelectric receivers is given in Patli's paper). However, in the steady-state, the polarization proves to be masked by the surface charges, and for this reason the incident radiation must modulated. As a result, the recording is realized using alternating current, while the background signal level is subtracted. Pyroelectric receivers are fabricated from inexpensive materials and operate at room temperature. However, the sensitivity of the existing pyroelectric IR receivers is considerably lower than for quantum receivers, and for this reason, cooling is also promising here.

The detection of thermally induced electrical charges in a pyroelectric becomes possible if the dielectric of the capacitor is a pyroelectric material close to the Curie-Weiss point, for example, triglycine-sulfate (TGS) at room temperature. A signal can be fed from a pyroelectric receiver to a CCD in two ways: connected a capacitor to the input MOS transistor on the same chip; create a pyroelectric film between the MOS transistor channel and the metal of the gate (i.e., insert it in series with the gate). These methods are essentially the same; the second one is more technologically complex, but makes it possible to obtain a more compact structure. The operational principle of the device consists in the following. The voltage produced by the pyroelectric receiver modulates the depth of the potential well in the MOS structure; the rate of thermally generated charge carrier transport to the nearest potential well of the CCD shift register of the least cross-section, but the deepest, is thereby modulated. The voltage V_0 is constant and chosen so that the depth of the potential well amounts to a few kT. The charge generation processes (primarily from surface states) keep the well practically filled with charge carriers. Charge drainage takes place through the potential barrier to the CCD channel. The voltages for the device so that the following conditions are met for a variable image signal, modulated by a special chopper: the amplitude is not limited by the dark current; the dark current reaches a level such that the signal modulation level amounts to practically 100%.

---

* The concept of creating hybrid CCD's based on pyroelectrics belongs to B.I. Sedunov.

An analysis of the noise properties of the device of [33] shows that as a first approximation, thermal noise introduced by the receiver and the input circuit plays the dominant role. In the typical case of an IR band CCD with receiving elements made of triglycine sulfate with an area of 10^{-5} cm^2 on SiO_2 with a thickness of 600 Å at 20 frames per second, the minimum temperature difference which can be resolved by the device can amount to about 0.3°K in a transmittance window of 8 to 12 micrometers. It should be noted that for the realization of the theoreticaly working characteristics in typical devices, it is necessary to provide for for a high degree of thermal insulation of the receiver so that it is not heated up by the substrate and there is no crosstalk interference between individual receiving elements arranged in a row.

SELECTED BIBLIOGRAPHY

12. "Infrakrasnyye methody v kosmicheskikh issledovaniyakh" ["Infrared Techniques in Space Research"], Translation from the English, Edited by V. Manno and J. Ring, Moscow, Mir Publishers, 1977.

17. Alfeyev V.I., "Sverkhvysokochuvstvitel'naya selektivnaya radiopriyemnaya sistema" ["An Ultrasensitive Selective Radio Receiving System"], U.S. Patent No. 3.381.225, issued 30 April 1968.

33. PROCEEDINGS OF THE IEEE: Topical Issue Devoted to Remote Infrared Sensing, 1975, Vol 63, No 1.

34. Nosov Yu.R., Shilin V.A., "Poluprovodnikovyye pribory s zaryadovoy svyaz'yu" ["Semiconductor Charge Coupled Devices"], Moscow, Sovetskoye Radio Publishers, 1976.

35. Stickle A., Nelson R., French B., Gudmunsen R., Shachter D., "Primeniye PZS dlya registratsii IK signalov i formirovaniya izobrazheniya" ["The Use of CCD's for Signal Recording and Image Generation"], TIIER [PROC. IEEE], 1975, Vol 63, No 1.

36. Sato Iwasa, "Hybrid CCD Infrared λ = 5μ" OPTICAL ENGINEERING, 1977, Vol 16, pp 233-237.

37. Alfeyev V.N., Bovina L.A., Karev A.A., Legezo S.L., Sedunov B.I., Stafeyev, V.I., "Gibridnyy PZS na λ = 8--14 mkm s priyemnymi HgCdTe elementani" ["Hybrid CCD's for a Wavelength of 8 to 14 Micrometers with HgCdTe Receiving Elements"], ELEKTRONNAYA TEKHNIKA, Seriya 10, Mikroelektronnyye Ustroystva [Microelectronic Devices], 1979, No. 3.

8225
CSO: 8144/1828

- END -